# Wearable Vital Signs Monitoring for Patients With Asthma: A Review

Lucy Taylor, Xiaorong Ding, *Member, IEEE*, David Clifton, and Huiqi Lu, *Member, IEEE*

***Abstract*—Worldwide, an estimated 461 000 people die from asthma attacks each year. While there remain treatments to alleviate asthma symptoms and reduce deaths, patient deterioration needs to be identified in sufficient time. To prevent asthma deterioration, patients need to be aware of personal and environmental triggers and monitor their asthma symptoms. The aim of this article is to provide a comprehensive review of the current state-of-the-art wearable sensors and devices that use vital signs for asthma patient monitoring and management. Among all vital signs, breathing rate and airflow sound are key indicators of asthmatic patients' health that can be measured directly using wearable sensors to provide continuous and constant patient monitoring or indirectly by estimations based on proven algorithms using electrocardiogram (ECG), photoplethysmogram (PPG), and chest movements. ECG and PPG signals are widely used in smart watches and chest bands, enabling easy integration of a more extensive body sensor framework for asthmatic exacerbation prediction. Other vital signs used in asthma patient monitoring include blood oxygen saturation, temperature, blood pressure, verbal sound, and pain responses. The use of wearable vital signs enabled a broad range of wearable sensor application scenarios for asthma monitoring and management.**


***Index Terms*— Asthma, breathing rate (BR), digital health, electrocardiogram (ECG), mobile health, patient monitoring, photoplethysmogram (PPG), sensors, wearable technology.**

## I. Introduction

WORLDWIDE, more than 300 million people are suffering from asthma, with around 461 000 expected deaths each year [1], [2]. In European countries, U.K. has the highest prevalence; approximately 12% of the U.K. population has been diagnosed with asthma [2], [3]. While asthma is a lifelong condition, most patients can be symptom-free with treatment and a self-management plan. However, approximately 5% of patients with asthma have a severe condition, where symptoms are usually hard to control [4]. Severe asthma is a complex heterogeneous disease entity with high morbidity and mortality.

As there are treatments to alleviate asthma symptoms (such as inhaled medication), many of these deaths are preventable, especially in lower income countries where access to diagnosis and treatment is limited [1]. Although some deaths will occur as a result of the rapid onset of symptoms, allowing little time for intervention, a large proportion of patients will slowly deteriorate across a number of days or even weeks [5]. If periods of decline are accurately identified early on in the development of symptoms, it allows ample time for intervention and reduces the chance of further deterioration, which can lead to death.

People with asthma can manage their condition by using a preventer inhaler every day and a reliever inhaler if their symptoms appear. The inhalers are typically loaded with drugs such as bronchodilators and corticosteroids to relax the muscles that constrict the airways and reduce inflammation in the lung.

There are two major types of inhalers: pressurized metered-dose inhalers (pMDIs) and dry powder inhalers [6]. The pMDIs deliver medication with a mix of propellant in a spray, which users need to shake and then apply pressure

Manuscript received 29 August 2022; revised 15 November 2022; accepted 17 November 2022. Date of publication 1 December 2022; date of current version 31 January 2023. The work of Lucy Taylor was supported by the Somerville College Scholarship Fund. The work of Xiaorong Ding was supported by the Medico-Engineering Cooperation Funds from the University of Electronic Science and Technology of China under Grant ZYGX2021YGLH005. The work of Huiqi Lu was supported in part by the Engineering and Physical Sciences Research Council (EPSRC) Healthcare Technologies Challenge Award under Grant EP/N020774/1, and in part by the Oxford John Fell Fund under Grant 0011028. The work of David Clifton was supported in part by the National Institute for Health Research (NIHR) Oxford Biomedical Research Centre (BRC) and in part by InnoHK Project Programme 3.2: Human Intelligence and AI Integration (HIAI) for the Prediction and Intervention of CVDs: Warning System at Hong Kong Centre for Cerebro-Cardiovascular Health Engineering (COCHE). For the purpose of open access, the authors has applied a Creative Commons Attribution (CC BY) license to any Accepted Manuscript version arising. The associate editor coordinating the review of this article and approving it for publication was Dr. Edward Sazonov. *(Corresponding author: Huiqi Lu.)*

Lucy Taylor and Huiqi Lu are with the Somerville College and the Department of Engineering Science, University of Oxford, OX2 6HD Oxford, U.K. (e-mail: lucygvt@yahoo.co.uk; yvonne.lu@eng.ox.ac.uk).

Xiaorong Ding is with the School of Life Science and Technology, University of Electronic Science and Technology of China, Chengdu 610056, China (e-mail: xiaorong.ding@uestc.edu.cn).

David Clifton is with the Department of Engineering Science, University of Oxford, OX3 7DQ Oxford, U.K., and also with the Oxford Suzhou Centre for Advanced Research, Suzhou 215000, China (e-mail: david.clifton@eng.ox.ac.uk).

Digital Object Identifier 10.1109/JSEN.2022.3224411

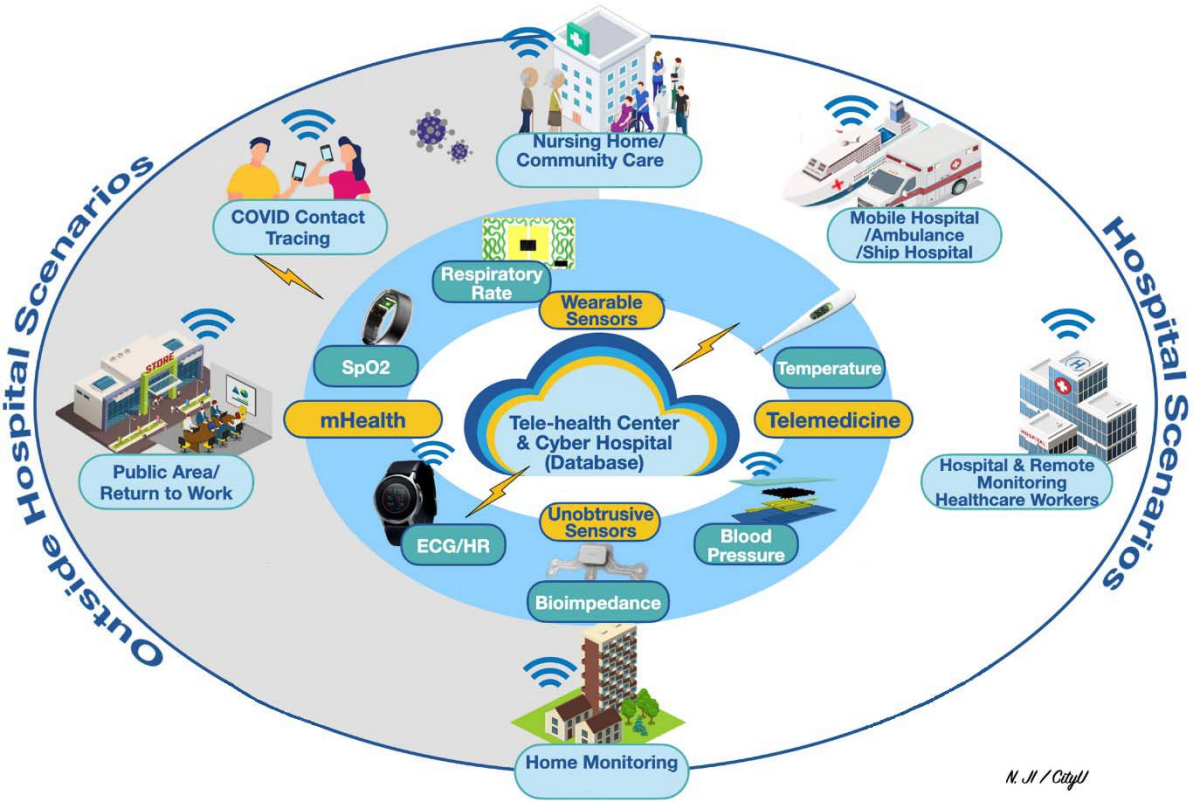


Fig. 1. Application scenarios of wearable devices and vital signs for monitoring patients with asthma. The original design concepts of this figure are borrowed from Dr. N. Ji [7] and Dr. R. Pettigrew's presentations at the IEEE Life Sciences Grand Challenge Conference held at the National Academy of Sciences in 2012 [8], [9], [10].

to dispense the medication. The dry powder inhalers are of different shapes, e.g., a disk-shaped device with a dose count indicator. Training and practice are required to ensure that patients use their inhalers correctly, which makes the delivery of medication challenging, especially for children and elderly individuals.

Individuals who have asthma can have their condition deteriorating due to various reasons, but the deterioration will normally follow one of two routes; the patient can either have their condition worsen slowly over a period of days or at a much faster rate within a few hours. For both the rapid and the slow onset of deterioration, the patient will experience a similar pathway of decline in their physiological health. Although they may not experience all of the symptoms at once, they will likely experience a combination of chest tightness, wheezing, breathlessness, and coughing fits [11] (due to asthma causing an inflamed airway). These symptoms will also be reflected in changes to the patient's vital signs, including their breathing rate (BR), heart rate (HR), and blood oxygen saturation [5].

People with asthma are likely to have triggers that will increase the likelihood of their condition deteriorating, where the combination of triggers is patient-specific. Some of the most common triggers include weather, pollution, pollen count, and exercise [12]. To prevent asthma deterioration, patients need to be aware of triggers and monitor their asthma symptoms [13].

Fig. 1 shows how patients with asthma can be monitored and managed inside and outside hospital scenarios. In the hospital scenario, patients are monitored by bedside equipment for their vital signs. Patients with severe asthma can be examined by computed tomography (CT) scans to identify bronchopulmonary aspergillosis or detect hypersensitive pneumonitis (mimic asthma) [14], [15]. However, there are only a few studies on the quantitative assessment of proximal airway structure changes in asthmatic adults [16], [17] and children [18], [19]. Moreover, due to radiation exposure and the size of the equipment, CT is not a standard of practice for asthma monitoring modality in hospital settings.

Although bedside equipment provides good patient monitoring, these devices are expensive, not portable, and require access to the main power supply. Therefore, the two main types of long-term monitoring systems for the deterioration of asthmatic symptoms outside of the hospital setting are asthma questionnaires and mobile-health applications. Patients can complete weekly questionnaires, such as the asthma symptom tracker (AST) [20], which uses a scoring system to assess the patient's asthma symptoms over the previous week. The system classifies the likelihood of deterioration based on the results of the questionnaire. Although the questionnaire can be helpful, there are several limitations—primarily, they rely on patients filling out the questionnaire accurately and reliably.

The intelligent alternative to questionnaires is mobile-health applications, which are helpful tools for online symptom tracking. SaniQ Asthma [21] is an application that acts as an online record of asthma-related medical history, including peak flow recordings and blood oxygen saturation. Medication can also be manually inputted, and local pollen count values

are included in the interface, enabling the app to predict when symptoms will likely worsen. Alternatively, Propeller [22] is a sensor that can be attached to the top of the patient's inhaler and links to an application on their smartphone, acting as a tracker and reminder for when to take their medication. The system also includes local weather and pollution levels to provide indications as to whether the patient's symptoms will deteriorate. Similarly, Smart Asthma [23] links a sensor attached to a patient's inhaler to the Smart Asthma smartphone application. In addition, a Smart Asthma spirometer can be attached to the patient's mobile phone to directly record peak flow measurements, and symptoms can be manually inputted to the application. This enables Smart Asthma to predict when their symptoms will deteriorate.

Although the above methods are useful for predicting patient stability, they at least in part rely on patients manually entering information such as medication usage or general feedback about their symptoms. As an asthmatic patient's condition deteriorates, there will be physiological indicators that can be measured in a more accurate manner. Therefore, an alternative method for predicting asthmatic patient deterioration would be to monitor vital signs using wearable technology and sensors. By measuring these vital signs continuously, patient deterioration could be identified before the patient reaches a critical condition, and timely medical intervention could prevent the need for the subsequent hospital admission. The vital sign measurements could also be used alongside the existing technology to provide a more accurate prediction.

In this article, we focus on reviewing vital signs and sensor technologies (with an emphasis on BR) and their applications that were either developed for people with asthma or can potentially be used to monitor people with asthma. Vital signs are critical in monitoring and managing the health conditions of people with asthma. Beyond the commonly used vital signs, such as BR, oxygen saturation, temperature, blood pressure, and pulse/HR, there are unique "markers" that relate to asthmatic patients, such as level of nitric oxide in their exhale, verbal sound, and pain responses.

## II. Vital Sign Representation of Patient Health for Asthmatics

Vital signs are widely used as indicators of patient health to continuously monitor and track patient stability. "Gold-standard" measurements of vital signs are the most accurate and are meant to represent their true values. However, most of the methods behind "gold-standard" measurements are invasive or require highly specialized equipment, often only available in clinical settings. Nevertheless, it is essential to understand these methods in patient monitoring, as they can be used to evaluate the accuracy of vital signs recorded from other wearable technologies. Vital signs include body temperature, blood pressure, blood oxygen saturation, heart rate, and BR.

### A. Gold-Standard Measurements for Vital Signs

*1) Body Temperature:* The "gold-standard" core body temperature measurement is through the use of a mercury thermometer, which is most commonly placed orally [24]. The in-ear temperature is higher than the oral measurement and cannot be used as an accurate gold-standard measurement. The normal physiological range for temperature is from 36.5 °C to 37.2 °C [25], which does not appear to be directly affected by an asthma exacerbation.

*2) Blood Pressure:* The "gold-standard" blood pressure measurement is performed using a mercury sphygmomanometer, which contains a cuff and a mercury manometer [26], [27]. Due to the environmental impact of mercury, modern sphygmomanometers use alternative manometers. When taking a measurement, the cuff is placed around the arm and inflated to occlude the arterial vessels, with the manometer recording the pressure of the cuff. The pressure is gradually reduced, increasing the arterial blood flow and leading to Korotkoff sounds, which can be separated into phases that occur at different levels of vessel occlusion. A trained practitioner can identify Korotkoff sounds and phases corresponding to systolic and diastolic blood pressure (with the values being read off the manometer).

The normal physiological range for a healthy adult's blood pressure is a systolic blood pressure of less than 120 mmHg and a diastolic blood pressure of less than 80 mmHg [25], which does not appear to change as a direct result of an asthma exacerbation.

*3) Blood Oxygen Saturation:* The "gold-standard" measurement for blood oxygen saturation is arterial blood gas (ABG) analysis [28], where a sample of blood is taken from a patient's artery and sent to the laboratory for ABG analysis. However, this is a highly invasive measurement technique that only provides intermittent monitoring, as each test requires a new sample of blood.

In clinical settings, a pulse oximeter is instead commonly used for continuous monitoring, from which a photoplethysmograph (PPG) signal is obtained [29]. During pulse oximetry, two different wavelengths of light are transmitted through a section of the body, and either the reflected or the transmitted signal is recorded. Traditionally, the two wavelengths of light used are red and near infrared (NIR). As oxygenated and deoxygenated, blood has different absorption spectra, and the received signal from the pulses of light can be used to determine the blood oxygen saturation [29].

The normal physiological range for a healthy adult's blood oxygen saturation ($SaO_2$) is between 95% and 100% [30], while for asthmatic patients experiencing an exacerbation, this range lowers to less than 90% $SaO_2$ [5].

*4) Heart Rate:* The "gold-standard" heart rate measurement is through the use of a 12-lead electrocardiograph (ECG) [31], where ten ECG electrodes are placed at specific locations on the chest. The most common electrodes used are Ag/AgCl, which are attached to the skin via the use of conductive gels. This reduces the impedance of the electrode–skin interface, so a higher quality ECG signal can be achieved [32]. Two electrodes are required to make a "lead," which acts as a transducer and converts the ionic potentials generated from the polarization phases during the cardiac cycle into an electrical potential. This electrical potential can then be processed and displayed on a monitor [33], from which features, such as the

QRS complex, can be identified, and the heart rate can be extracted.

The normal physiological range for a healthy adult's heart rate is from 60 to 100 beats/min [25], while for asthmatic patients experiencing an exacerbation, this range increases to greater than 120 beats/min [5].

*5) Breathing Rate:* The clinical "gold-standard" measurement for BR derives from a capnography waveform [34], which uses the absorption spectra of carbon dioxide ($CO_2$). By passing infrared radiation through exhaled air, the concentration of $CO_2$ can be measured [35]. As this concentration will change through periods of exhalation and inhalation, a waveform of $CO_2$ concentration against time can be plotted from which the BR can be estimated. In clinical settings, the industry-standard method is instead more commonly used, where a stopwatch records a time over which breaths are manually counted [34].

The normal physiological range for a healthy adult's BR is from 12 to 20 breaths/min [25], while for asthmatic patients experiencing an exacerbation, this range increases to greater than 30 breaths/min [5].

*6) Airway Sound:* The stethoscope performs the "gold-standard" airway sound measurement to identify wheezing, stridor, rhonchi, and crackle sound in the lung. Wheezing is a high-pitched whistling sound that can be heard from patients at breath out. This sound can be heard in the lung using a stethoscope when airways are narrowed due to bronchospasms and/or inflammation. A stridor sound is a high-pitched harsh sound that can be heard without the use of a stethoscope. Stridor sound appears when there is disrupted airflow or obstruction. For children with asthma, stridor sounds are often a joint effect caused by croup (a rare viral condition), pertussis (whooping cough), and epiglottitis (airway swollen caused by infection or physical trauma). For adults, stridor occurs due to vocal cord dysfunction.

### B. Vital Signs for Monitoring Asthmatic Patient Deterioration

Obtaining clinical-standard vital sign measurements based on the "gold-standard" and industry-standard methods is not practical for the continuous monitoring required to predict patient deterioration. Therefore, measuring vital signs using wearable devices provides an excellent opportunity for novel approaches to chronic respiratory health monitoring. BR is one of the key indicators of asthmatic patient health. Blood oxygen saturation and heart rate could also be used as indicators of asthmatic patient stability, as they are both affected by an asthma exacerbation, but the BR is the preferred monitoring method in the majority of applications. BR is broadly used because it can be observed directly (such as by looking at the movement of the chest or hearing the breathing sound) or extracted from either the ECG or PPG signals. If the BR is extracted from signals measuring other vital signs, then the raw data from these vital sign signals can also be recorded and used simultaneously with the BR at little extra effort. This would allow heart rate and blood oxygen saturation to be easily incorporated into a more extensive model for predicting deterioration in asthmatic patients who could be developed in the future. Other vital signs used in asthma patient monitoring include blood oxygen saturation, temperature, blood pressure, verbal sound, and pain responses.

## III. Using ECG and PPG Signals to Measure BR

### A. BR Extraction From Vital Signs

To continuously monitor patients with asthma, measuring the BR directly using capnography is impractical [35]. In wearable device applications, the BR is commonly estimated using recordings of other vital signs, such as ECG and PPG signals. This section focuses on reviewing how BR is measured using ECG and PPG signals.

*1) BR Extraction From an ECG Signal:* A patient's BR can be extracted from an ECG signal, which shows the changing electric potentials of the heart over the course of the cardiac cycle. There are several ways of extracting the BR from an ECG signal: using R–R interval modulation [caused by respiratory sinus arrhythmia (RSA)], using baseline wander, or using R-peak amplitude modulation [36].

RSA is a physiological condition present in everyone but is particularly pronounced in children and younger adults. As the heart rate decreases during patient exhalation and increases during inhalation, the R–R interval (time between successive R peaks) is modulated by the BR. Algorithms used to extract the breathing rate from an ECG signal are summerised in Table I.

RSA-based methodologies can be used to estimate the BR from the R–R interval modulation in the ECG signal. As demonstrated by Helfenbein et al. [37] and Ruangsuwana et al. [38], the R–R interval can be found from the time difference between similar features in consecutive QRS complexes, from which the instantaneous heart rate (IHR) can be extracted. Using cubic splines to interpolate between values of the IHR, the breathing waveform can be displayed, and the BR can be found from the frequency of this waveform. Nayan et al. [36] instead followed a different pathway using an RSA-based methodology. The ECG signal was initially preprocessed to remove the baseline wander and the high-frequency components (using a Savitzky–Golay filter), with the R-peaks identified using an ECG demo peak detection function developed by Chernenko. From this signal, the BR can be estimated. In addition, the signal quality was assessed through the partial autocorrelation of the RSA wave with an autoregressive (AR) model.

Alternative methods for estimating the BR from ECG signals involve direct R-peak detection. Once the R-peaks are identified, the instantaneous R–R interval can be found and plotted against time. From this sinusoidal waveform, the BR can then be estimated.

Along this concept, Wang et al. [39] used a method for R-peak detection involving three discrete criteria. The ECG signal was partitioned into a series of samples, and for each reference sample, another two samples were found at 0.03 and 0.08 s (as the time difference between these samples corresponds to the average length of time for a QRS complex). The first criterion found the slopes of the lines between the reference sample and the two other samples, with the gradients of these lines calculated. A "slope difference" value can then be calculated, which if above a certain threshold classifies the

TABLE I
SUMMARY OF ALGORITHMS USED TO EXTRACT THE BREATHING RATE FROM AN ECG SIGNAL

| Lead Author | Method for Extracting the Breathing Rate | Overview of algorithm |
|---|---|---|
| E. Helfenbein [37], and R. Ruangsuwana [38] | R-R interval modulation. | Cubic splines to interpolate between consecutive values of the instantaneous heart rate hence extract the breathing waveform. |
| E. Helfenbein [37] | R-peak (QRS) amplitude modulation. | Cubic splines to interpolate between consecutive QRS amplitudes. Apply a high pass filter to the ECG signal, calculate the RMS value then apply a smoothing filter. |
| E. Helfenbein [37] | High frequency signals from chest and intercostal muscles during respiration cycle. | |
| R. Ruangsuwana [38] | Baseline wander. | Cubic splines to interpolate between consecutive R-peak amplitudes (to get R-R curve envelope). |
| N. A. Nayan [36] | R-peak detection*. | R-peak identification, then partial autocorrelation of RSA waveform with an autoregressive model for signal quality assessment. |
| Y. Wang [39] | R-peak detection*. | |
| X. Tang [40] | R-peak detection*. | R-peak detection using a threshold value applied to the gradient of the signal. |
| N. Ravanshad [41], and X. Zhang [42] | R-peak detection*. | Three-state delta modulator with a local maximum point algorithm to detect R-peaks. |
| K. Zhao [43] | R-peak detection*. | Level-crossing method applied to the output of an ADC to identify R- peaks. Band pass filter before applying a bilateral filter and a "QRS watchdog". |
| C. O'Brien [44] | R-peak amplitude modulation. | Filter ECG signal, detect R-peaks then plot their amplitude against time. |

* R-R interval identification and modulation

reference sample as a peak. The second criterion sets a series of inequalities that need to be satisfied (to ensure that the peak has sufficient steepness on either side), with the third criterion requiring the height of the current peak to be above 0.4 times the average of the previous eight peaks identified (to ensure that the peak is not that of a T or P wave). If all three criteria are met, then an R-peak has been identified.

Along with a similar approach, Tang et al. [40] used a three-state delta modulator, where the delta voltage is generated by subtracting the feedback voltage from the input ECG signal. The signal output of the modulator describes whether the delta voltage is greater than, lower than, or between the two reference voltages. A local maximum point algorithm is then used to detect the rising and falling edges of the R-peak: if the number of consecutive rising segments is higher than a set threshold value, it is considered an R-peak. If the number of consecutive falling samples is also higher than the threshold value, the whole QRS complex has been detected.

R-peaks can also be detected using a novel level-crossing-based method [41]. The output signal from an analog-to-digital converter is defined by two quantization levels [called a level crossing analog-to-digital converter (LC-ADC)], between which the signal lies. If the signal leaves the range between the levels, the levels change by value $k$ to ensure that the signal remains within the range. The value of $k$ can be set to one least significant bit (LSB) or higher numbers of LSBs (which help to filter out noise). The peaks of the signal are detected from the change in value of the level crossing signal, from which the R-peaks can be identified. As the difference between the values of the level crossings is constant, the time difference between level crossings can be used as a gradient indicator of the peak. Around the detected peak, the sum of the time intervals of a constant window of the level crossings can be found, and a threshold applied to the value—if this duration of the peak is less than a certain value, then the peak is that of an R-peak. Dead-time zones between successive peaks are also used to prevent T-waves from being falsely identified as R-peaks. Zhang and Lian [42] also used a level-crossing-based ADC to process the ECG signal, enabling the identification of R-peaks from setting threshold parameters.

Zhao et al. [43] instead conducted R-peak identification using three discrete steps. Initially, the signal is preprocessed using a bandpass filter to reduce noise and help identify potential R-peak candidates. A bilateral threshold is then applied to determine the R-peaks from the possibilities found in the previous step. A "QRS watchdog" is finally applied, using a search-back function to identify missing R-peaks from long time gaps between successive R-peaks.

Baseline wander of the ECG signal can occur from general motion artifacts but also as a result of the chest rising and falling during the respiration cycle (relevant only to ECG electrodes that are placed directly onto the skin and not from other technology such as smart watches). From the ECG trace, Ruangsuwana et al. [38] showed that this R–R curve envelope can easily be found by interpolation of consecutive R-peaks using cubic splines (or by using the ECG mean), from which the breathing waveform, and hence the BR, can be estimated.

The R-peak amplitude modulation during the breathing cycle can also be used to extract the BR [44]. Throughout the breathing cycle, the distance between the chest wall and the heart changes, as does the impedance of the chest due to the varying volume of air within the lungs. These physiological factors manifest as changing QRS amplitudes. Initially, the baseline wander needs to be filtered out (achieved using a 20th order, high pass, linear phase, and finite-impulse response (FIR) filter) and the R-peak locations detected (using a Hilbert transformation-based QRS detector). After anomalous peaks are rejected, the remaining R-peak amplitudes can be plotted against the time at which they occur. After low-pass filtering of this signal, a smooth ECG-derived respiratory (EDR) estimate (from which the BR can be estimated) can be plotted.

Along a similar methodology, QRS amplitude modulation can be used to estimate the BR from an ECG signal [37]. Initially, a QRS detector was used, and the amplitude of the QRS complex was recorded. This amplitude can be plotted against time, and cubic splines can be used to interpolate between consecutive values to obtain the EDR waveform. By also employing a bandpass filter with suitable cutoff frequencies (corresponding to realistic BR limits) to the interpolated signal, the BR can be extracted.

Similar to the above methodologies, but for ECG electrodes placed directly onto the chest, QRS amplitudes can be found from which cubic splines can be used to interpolate between consecutive values [37]. By also employing a bandpass filter with suitable cutoff frequencies (corresponding to realistic BR limits) to the interpolated signal, the BR can be extracted. In addition, the intercostal chest muscles and diaphragm produce high-frequency signals overlaid on the ECG recording, which correspond to their muscle activity throughout the respiratory cycle. Therefore, a breathing waveform can be extracted by applying a high-pass filter (with a cutoff frequency of 250 Hz) and calculating the rms value of the signal using a sliding window [37]. However, this would still include residual high-frequency fragments of the QRS complex; by performing QRS signal to find the location of the QRS complexes and then applying a smoothing filter over the corresponding times in the breathing waveform signal, the remaining QRS peaks can be filtered out.

*2) BR Extraction From a PPGSignal:* Although pulse oximetry is used to measure blood oxygen saturation, the heart rate, and hence BR, can also be extracted from the PPG signal. The heart rate can be extracted due to the pulsatile nature of blood flow through the body, from which the BR can be extracted due to RSA.

There are many different methods to extract the BR from the PPG signal. They all follow a similar structure: extracting the BR envelope from the overall signal, removing the dc offset, and then using a variety of peak detection methods to establish the BR. Algorithms used to extract the breathing rate from a PPG signal are summerised in Table II.

Fusco et al. [45] developed an algorithm for BR extraction based on the empirical mode decomposition (EMD), which decomposes the PPG signal into different frequency-and-amplitude modulated signals using intrinsic mode functions (IMFs). The local maxima and minima of the signal are identified from which the envelopes of the signal can be interpolated. The mean is then removed to account for any dc offsets, and a smoothing filter is applied (as an initial step) to reduce the strength of unwanted signals such as motion artifacts. The lowest frequency component of the processed signal corresponds to the respiratory waveform, from which the BR can be extracted. Ambekar and Prabhu [46] took a similar approach but first added white noise uniformly to the signal before first decomposing it into IMFs and then performing an ensemble EMD (EEMD). The ensemble mean for the IMFs falling in the frequency range of 0.2–0.33 Hz is then used to calculate the final BR.

Along with a similar methodology, Li et al. [47] first decomposed the PPG signal into a series of Gaussian basis functions. The optimal parameters for the basis were found through optimization of the least-squares error using the steepest descent method to find the minimization. The Gaussian basis can then be processed using the Hilbert transform, and this representation of the signal can be smoothed using the Shannon energy envelope approach. The location of the second highest peak along the frequency axis from the Shannon energy envelope corresponds to that of the BR.

TABLE II
SUMMARY OF ALGORITHMS USED TO EXTRACT THE BREATHING RATE FROM A PPG SIGNAL

| Lead Author | Overview of Algorithm |
|---|---|
| A. Fusco [45] | Empirical Mode Decomposition of the PPG signal into the Intrinsic Mode Functions. |
| R. Mitali [46] | White noise addition to the signal before finding the Intrinsic Mode Functions through Ensemble Empirical Mode Decomposition. |
| D. Li [47] | Gaussian basis decomposition of the PPG signal before applying the Hilbert Transform and the Shannon Energy Envelope Approach. |
| S. Fleming [48] | Autoregressive model of the PPG signal to find the pole-zero plot and corresponding breathing-rate pole. |
| L. Nilsson [49] | Peak identification using a third-order Butterworth filter. |
| P. Leonard [50] | Continuous Wavelet Transforms. |
| T. Freeman [51] | Pulse identification and extraction of landmark features. |

Alternatively, Fleming and Tarassenko [48] developed an algorithm based on an AR model. Initially, the recorded PPG signal is downsampled. This helps to remove any of the signal components corresponding to cardiosynchronous fluctuations and reduce inaccuracies in the phase angles identified later. Any dc offset in the signal is also removed. The downsampled signal is then resampled, with a decimation algorithm applied to act as an antialiasing filter. Standard AR modeling is then applied

$$x(n) = -\Sigma_{k=1}^{p} a_k x(n-k) + e(n). \quad (1)$$

Taking $e(n)$ (the noise term) as the input and $x(n)$ as the output, the transfer function from the AR model can be expressed as a fraction, with the poles in the denominator and the zeros in the numerator. From this, a pole-zero plot can be formed, and the pole with the largest amplitude (also within the expected frequency range for BR) can be identified. Setting a threshold to 95% of this value, the lowest frequency pole with an amplitude above the threshold value corresponds to the BR.

Peak detection on the PPG signal also provides more straightforward processing to extract the BR. Nilsson et al. [49] simply filtered their PPG signal using a third-order Butterworth bandpass filter with cutoff frequencies at 0.1 and 0.3Hz, before using peak identification to find the times of individual breaths. From this, the BR can be extracted by the inverse of the average time between consecutive peaks. As shown by Leonard et al. [50], continuous wavelet transforms (CWTs) can also be used to decompose the PPG signal into two bands, of which the frequency of one corresponds to the BR. In addition, a scalogram can be plotted from the CWT, which can be projected into the amplitude–time domain (to obtain the ridge amplitude perturbation (RAP) signal) or into the frequency–time domain (which obtains the ridge frequency perturbation (RFP) signal). Another wavelet transform can then be applied to the RAP and RFP signals, from which the BR can also be extracted.

Although Freeman [51] did not apply this methodology using an algorithm but instead manually identified the key features of the PPG signal; it presents an alternative concept

TABLE III
SUMMARY OF WEARABLE ECG SENSORS

| Lead author or product name | Type of electrode | Location of sensors | Device which sensor is integrated into | Development for asthma monitoring? | Potential for asthma monitoring? | Clinically proven? | Mobile Apps |
|---|---|---|---|---|---|---|---|
| Z. Zhang [52] | Standard electrodes. | Chest | Wearable shirt. | No | Low | No | No |
| C. Park [53] | Insulated bioelectrdoes. | Chest | Wearable shirt. | No | Low | No | No |
| R. Fensli [54] | Ag electrodes (in a novel sensor). | Chest | Directly to the skin using conductive hydrogel. | No | Medium | No | No |
| D. Yamamoto [55] | Ag electrodes integrated into a PET film. | Chest | Directly to the skin using a commercially available ion gel. | No | Low | No | No |
| Y. Yamamoto [56] | Ag electrodes integrated into a PET film. | Chest | Directly to the skin using a bio-compatible adhesive layer. | No | Low | No | No |
| N. G. Hallfors [59] | Reduced graphene-coated Nylon[1] electrodes. | Wrist and neck | Directly to the skin. | No | Low | No | No |
| E. Nemati [60] | Capacitive electrodes. | Chest | Placed on skin via the use of a cloth. | No | Low | No | No |
| E. Sardini [61] | Ag electrodes. | Chest | Band/belt. | No | Low | No | No |
| PhysioDroid [62] | Ag electrodes. | Chest | Band/belt. | No | Medium | No | Yes |
| LifeMonitor [63], [64] | Textile-based electrodes. | Chest | Band/belt. | No | Medium | No | No |
| P.S.Pandian [65] | Ag electrodes. | Chest | Wearable vest. | No | Low | No | No |
| M. Yapici [66] | Graphene-coated Nylon[1] electrodes. | Neck or wrists | Integrated into the inside of elastic bands. | No | Medium | No | No |
| Apple Watch [70],[71] | Not specified and varied in different models. | Wrist | Integrated into a watch interface on the back of the watch and the watch face | No | Medium | Yes | Yes |
| Withings Move ECG Watch [72] | Ag electrodes | Wrist | Integrated into a watch interface on the back of the watch and the watch face. | No | Medium | Yes | Yes |
| KardiaMobile [73],[74] | Ag electrodes | Two fingers from each hand | A small hand-held device is used only when a recording is to be made. | No | High | Yes * | Yes |

*FDA approved

for extracting the BR. The PPG signal was initially segmented into pulses, and landmarks were identified (the landmarks, including the start point, endpoint, systolic peak, and diastolic peak of each pulse). Pulses were individually evaluated for suitability, and the BR was calculated from the time difference between the foot and the systolic peak.

### B. Commercially Available Wearable ECG and PPG Monitoring Technologies

*1) Wearable ECG Sensors:* As described in Section II-A4, the "gold standard" for measuring the heart rate is a 12-lead ECG, where the electrodes are attached directly to the skin and wired to a bulky monitor for display and processing. However, alternative wearable technology must be implemented for ambulatory monitoring of ECG as patients follow their regular daily routine. To achieve this, traditional ECG sensors can instead be integrated into a wearable shirt, and the recorded signal can be transmitted wirelessly to an external control unit for processing [52]. A summery of wearable ECG Sensors is listed in Table III.

Park et al. [53] were able to integrate insulated bioelectrodes (similar to the "gold-standard" electrodes but without the need for skin preparations, gels, or adhesives) into a wearable shirt from which to record the ECG signal.

Fensli et al. [54] attached their ECG electrode directly onto the chest using a conductive hydrogel, which has an integrated wireless transmitter to send the signal to a handheld device for processing. The electrode itself has two electrical conducting points to be attached to the skin, with the resulting patch resembling a plaster. Traditional Ag electrodes can also be integrated into an in-plane polyethylene terephthalate (PET) film, as demonstrated by Yamamoto et al. [55]. The ECG electrodes are screen-printed on the bottom surface of the PET film and are directly attached to the chest using a commercially available ion gel.

Yamamoto et al. [56] instead used biocompatible materials to attach the traditional Ag ECG electrode directly onto the chest. A mixture of ethoxylated polyethylenimine and polydimethylsiloxane created the adhesive layer with carbon nanotubes incorporated to improve the layer's adhesion and conductivity. Hallfors et al. [59] took the alternative approach of creating a new fabric sensor made from Nylon[1] and coated in reduced graphene oxide. The reduced graphene oxide can be attached to the Nylon[1] as a uniform coating through the aqueous solution it is suspended in, with the resulting fabric being soft, flexible, and electrically conductive. The electrodes can then be placed on the neck and the wrists to record the ECG signal.

Capacitive ECG electrodes can also be placed directly onto the skin, which transfers the electric charge from the cardiac cycle along the capacitive path made between the skin, the insulation layer, and the metal-plate sensor [60]. Two electrodes are placed on the chest, with a third electrode placed on the right hip used as the ground electrode to create the two-lead ECG recording.

Similarly, ECG electrodes can be integrated into bands worn around the chest. The recorded signal passes through a small control unit integrated into the band before being wirelessly transmitted to an external computer for further processing [61]. PhysioDroid is a two-lead ECG system integrated into a band worn around the chest. PhysioDroid also has a smartphone

[1]Registered trademark.

application that displays ECG signals directly on the patient's phone [62]. Another commercial alternative is the LifeMonitor (which is also FDA 510k approved), where ECG electrodes are integrated into a band worn around the chest [63], [64]. ECG electrodes can also be incorporated into a belt within a vest, with the connective wires incorporated as a smart textile into the fabric of the underlying garment [65].

Yapici and Alkhidir [66] instead integrated a novel ECG electrode into elastic bands that can be worn either around the neck or wrists. The electrodes are made by dipping sections of Nylon[1] textile into a graphene oxide suspension, thermally treating the resulting material, and then dipping it in hydrogen oxide. The treated Nylon[1] is cut into 3 × 6 cm pieces, which are glued onto larger pieces of cotton fabric and then sewn onto the elastic bands (which are used to ensure good contact between the skin and the electrodes). As the electrodes are attached to the inside of the bands, metallic snap fasteners are used to electrically connect them to the outside of the bands, where the circuitry (for processing and transmitting the signal) is attached.

In addition, the ECG signal can be recorded through the use of wearable technology around the wrist integrated into smart watch interfaces. Both the Apple Watch (Series 4, 5, and 6) [70], [71] and the Withings Move ECG watch [72] have ECG sensors integrated into the hardware and operate on the same principle. The watches have electrode sensors placed on the back of the watch (so that they are in contact with the wrist onto which the watch is placed) and another sensor on the front face of the watch. For the Apple Watches, this front sensor is the "Digital Crown" on the side of the watch, and for the Withings Move ECG watch, this sensor is in the form of a metal disk around the front of the watch face. When the wearer wishes to make an ECG recording, they connect the watch to a designated app (specific to each watch) and place their opposite hand (to the one wearing the watch) on the front sensor for 30 s. As the contacts between the electrodes on the watch, the wrist wearing the watch, and the other hand create a loop, this technology acts in the same way as a traditional single-lead ECG recording. The signal is transmitted wirelessly from the watch to the app, which is then able to process the signal and display the ECG trace in a similar manner to that of the "gold standard."

Another example is the KardiaMobile device, which can record ECG signals using Android and iOS apps on mobile phones [73]. This portable device consists of two sensor pads, where the user places two fingers from each hand, as shown in Fig. 2(c). In comparison, iWatch is a one-lead ECG, and KardiaMoble has one-, six-, and 12-lead versions. The six-lead version has two ECG sensors on the top for fingers and one on the bottom to contact the skin of the left leg, delivering ECG leads I, II, III, aVL, aVR, and aVF [74]. The 12-lead version is currently under clinical trial. KardiaMobile has been clinically approved by the U.K. National Institute for Health and Care Excellence and is available to purchase without needing a doctor's subscription.

*2) Wearable PPG Sensors:* As demonstrated in Section III-A2, the BR can be extracted from a PPG

(a) (b) (c)

Fig. 2. Asthmatic monitoring using ECG. (a) Apple iWatch [58]. (b) Withings watch [59]. (c) KardiaMobile ECG monitor [74].

waveform. The PPG signal is traditionally recorded using a pulse oximeter attached to the finger connected to large monitors using wires [76]. Although this is the most accurate method for taking a pulse oximetry reading, it requires close proximity to the large monitors and control units, so it is not suitable for ambulatory monitoring of patients. Therefore, wearable pulse oximetry alternatives are required.

Wireless versions of traditional pulse oximetry sensors can instead be attached to different parts of the body, with the signals being transmitted via Bluetooth to a remote-control unit for analysis and extraction of the BR. Reflectance-type pulse oximeter sensors can be attached to the tip of the finger or to the forehead (using double-sided sticky tape and an elastic headband) [77]. The sensors can alternatively be directly integrated into devices that can be worn on the legs (BSX Insight) [78], thigh (Humon Hex) [79], and earlobe (Lumafit) [83]. In addition, Chetélat et al. [80] were able to embed both PPG and ECG sensors into a wearable vest, with the PPG sensors containing four optical channels. A summary of wearable PPG sensors are listed in Table IV.

Furthermore, PPG sensors can be integrated into smart rings, such as the Oura ring [81]. Pulse oximetry sensors are embedded into the inside of the ring, and the resulting PPG waveform is transmitted to an application on a smartphone for processing using in-built algorithms. Currently, the Oura ring can only measure the BR, while the user is sleeping, as this period has a lower motion artifact.

Pulse oximetry sensors can also be integrated into smart watches or devices worn on the wrist. The FDA has approved some of these sensors as medical monitoring devices, such as the Masimo sensor [82]. This sensor has similar operating principles and design to the "gold-standard" sensor used in clinical settings—it is a pulse oximetry sensor that is attached to the finger. In order to make the overall device wireless, the sensor is attached via a short wire to a small control unit that in turn is attached to the wrist using a strap.

The control unit is then able to send the acquired PPG signal to an external server for processing.

Alternatively, BioBeats is a smart watch with pulse oximetry sensors embedded into its hardware for PPG monitoring on the wrist [84]. The Fitbit Charge HR is another similar technology that uses PPG sensors integrated into a device worn on the wrist [85], [86]. The Fitbit Charge HR uses PurePulse, their patented technology in the form of a traditional pulse oximeter, pulsing a light-emitting diode onto the skin and recording the

TABLE IV
SUMMARY OF WEARABLE PPG SENSORS

| Lead author or product name | Location of sensor placement on body | Device which sensor is integrated into | Development for asthma monitoring? | Suitability for asthma monitoring? | Clinically proven? | Mobile Apps |
|---|---|---|---|---|---|---|
| W.S. Johnston [77] | Tip of the finger, and forehead. | Velcro strap, and double-sided adhesive with elastic headband. | No | Low potential | No | No |
| BSX Insight [78] | Leg | Band. | No | Low potential | No | Yes |
| Humon Hex [79] | Thigh | Band. | No | Medium potential | Yes | Yes |
| O. Chételat [80] | Chest | Wearable vest. | No | Low potential | Yes | Yes |
| Oura Ring [81] | Finger | Inside of a ring. | No | High potential | No | No |
| Masimo Sensor [82] | Tip of finger. | Clip connected to a strap around the wrist. | No | Medium potential | Yes * | No |
| Lumafit [83] | Earlobe | Fitted around ear. | No | Low potential | No | Yes |
| Biobeats [84] | Wrist | Smart watch. | No | Medium potential | Yes * | No |
| Fitbit Charge HR [85],[86] | Wrist | Fitness strap. | No | Medium potential | Yes | Yes |
| K. Lee [88] | Wrist | Strap. | No | Low potential | No | No |
| S. Browne [89] | N/A | Back of a smartphone. | No | Medium potential | Yes * | Yes |

* FDA approved

reflected waveform [87]. The Fitbit Charge HR has an in-built algorithm to extract the heart rate from the PPG signal, from which the BR can be extracted. As demonstrated by Lee et al. [88], pulse oximetry sensors can also be integrated into a simple watch strap, where the PPG signal is extracted from the radial and ulnar arteries. To minimize the noise signal integrated into the PPG waveform, the inside of the watch strap is lined with a conductive fabric that also connects to the ground, serving as a shield to the sensors.

Waveform is transmitted to an application on a smartphone for processing using in-built algorithms. Currently, the Oura ring can only measure the BR, while the user is sleeping, as this period has a lower motion artifact.

Pulse oximetry sensors can also be integrated into smart watches or devices worn on the wrist, as shown in Fig. 3. The FDA has approved some of these sensors as medical monitoring devices, such as the Masimo sensor [81]. This sensor has similar operating principles and is designed to the "gold-standard" sensor used in clinical settings—it is a pulse oximetry sensor that is attached to the finger. In order to make the overall device wireless, the sensor is attached via a short wire to a small control unit that in turn is attached to the wrist using a strap. The control unit is then able to send the acquired PPG signal to an external server for processing.

Alternatively, BioBeats is a smart watch with pulse oximetry sensors embedded into its hardware for PPG monitoring on the wrist [82]. The Fitbit Charge HR is another similar technology that uses PPG sensors integrated into a device worn on the wrist [83], [84]. The Fitbit Charge HR uses PurePulse, their patented technology in the form of a traditional pulse oximeter, pulsing a light-emitting diode onto the skin and recording the reflected waveform [85]. The Fitbit Charge HR has an in-built algorithm to extract the heart rate from the PPG signal, from which the breathing rate can be extracted. As demonstrated by Gorny et al. [86], pulse oximetry sensors can also be integrated into a simple watch strap, where the PPG signal is extracted from the radial and ulnar arteries. To minimize the noise signal integrated into the PPG waveform, the inside of the watch strap is lined with a conductive fabric that also connects to the ground, serving as a shield to the sensors.


Fig. 3. Asthmatic monitoring using PPG. (a) Oura ring [75]. (b) Masimo sensor [68]. (c) Fitbit Charge HR [69]. (d) Biobeats [70].

Furthermore, smartphones can have pulse oximetry sensors embedded into them, where the PPG signal is obtained by the user placing their index finger on the sensor [87]. The phone then takes a reading and uses an application on the phone for signal processing. Although it would not provide continuous monitoring in the same way that the other wearable sensors can, signal processing can be achieved directly on the smartphone app, thus making it unnecessary to transmit the signal elsewhere.

## IV. COMMERCIALLY AVAILABLE AND EMERGING WEARABLE TECHNOLOGIES

In the past ten years, wearable and contactless monitoring technologies have started shaping the new digital health era for monitoring and managing people with asthma. Many emerging wearable technologies have been developed and have become commercially available. These technologies can be broadly defined as contact and noncontact monitoring.

There are four main types of noncontact monitoring, including camera-based respiratory monitoring (infrared thermography or video), ultrasound-based monitoring, remote plethysmography, and radar-based respiratory monitoring (continuous wave Doppler radar, laser Doppler vibrometer radar, ultrawideband radar, and frequency-modulated continuous-wave radar).

While noncontact monitoring can provide patients with more comfort, especially for long-term monitoring, the majority of the digital health solutions that are available in the market are based on contact sensor technologies.

This section focuses on the most promising methods for measuring the breathing rate and airflow sounds, enabling asthmatic patients to be monitored in a nonclinical setting. Resistive and capacitive sensors can be integrated into smart textiles, wearable vests, or placed directly onto the skin to measure either the breathing rate or other vital signs associated with breathing.

### A. Skin Contact Wearable Sensors, Smart Textiles, and Wearable Vests to Measure the Breathing Rate

*1) Skin Contact Wearable Sensors:* Patients' breathing rates can be measured directly without needing a capnograph, due to emerging sensor technologies and innovations in material sciences.

The RespiraSense sensor takes the approach of applying the sensors directly to the skin, instead of via a wearable vest or being integrated into a smart textile garment [34]. The RespiraSense sensor is applied to the chest area using medical-grade adhesive, which in turn is attached to a small control unit that can be clipped onto items of clothing using thin wires. The sensors themselves consist of piezoelectric films organized into an array and can measure deformations in the relative angles between the thoracic and abdominal surfaces.

These deformations are then converted into an electric signal. The control unit consists of an in-built algorithm, a Bluetooth transmitter, and an accelerometer, allowing the breathing rate to be directly extracted from the signal. In addition, the accelerometer is used to reject motion artifacts from the signal and improve the accuracy of the calculated breathing rate. The Bluetooth transmitter is then able to send the signal to external systems for storage.

A similar methodology is demonstrated by Chu et al. [91], where a pair of sensors are attached directly to the skin around the circumference of the ribcage and abdomen using a double-sided adhesive. The sensors are made from a piezoresistive metal film set in a silicone elastomer substrate, with their changes in strain recorded to measure the breathing rate. The novel aspect of these sensors is the use of the technology behind the "Shrinky Dinks" toy (which consists of pieces of plastic that shrink considerably in size when they are heated up in the oven) when creating corrugation in the metal film [92]. In addition to the breathing rate, Chu et al. [91] extracted the respiration volume from the output of the sensors.

In clinical settings, the respiration volume is recorded using the "gold-standard" method simultaneously with the measurements from the skin sensors, allowing a calibration model between the two measurements to be created as each patient went through a set of prescribed breathing exercises. It was only necessary to complete this procedure once for the respiratory volume to then be estimated from any future measurements from the sensor signal.

*2) Smart Textiles and Wearable Vests:* The term smart textiles refer to a group of products in which electronic components are embedded (or sewn) into an existing textile or fabric. These innovative textiles can be used in patient monitoring applications, such as body movement, blood pressure, temperature, and breathing rate. By using smart textiles and incorporating various sensors into the vest-like items of clothing, there are several exciting innovations in wearable vests for breathing rate measurement and monitoring.


Fig. 4. (a) Bioharness [90]. (b) Technology based on ShrinkyDink toys [91].

As shown in Fig. 4, BioHarness 3.0 is one such technology in which a capacitive pressure sensor (operating at 25 Hz) is integrated within a vest to measure the changes in torso circumference as the patient inhales and exhales [90], [93]. An algorithm within the sensor converts the recorded pressure signal into a sinusoidal waveform, which can then be exported wirelessly to a remote server to be processed. The resulting signal is first resampled at 250 Hz. After the mean value is removed, a third-order Butterworth bandpass filter with cutoff frequencies at 0.5 and 1 Hz is applied for signal normalization using the absolute value of the waveform. This enables easy identification of the peaks associated with the breathing rate, with the time difference between successive peaks used to estimate the instantaneous breathing rate.

Another smart textile is formed when a foam-based version of polypyrrole (PPy) is sewn into an existing fabric [94]. PPy is a type of conducting electroactive polymer (CEP) used because it does not change the mechanical properties of the material it is integrated into. For use in a breathing rate sensor, PPy is sewn into the pocket of a T-shirt. As the patient inhales and exhales, the material is compressed and stretched, changing the electrical conductivity of the PPy. Two-wire leads can then be attached to either end of the sensor, and the resulting changes in voltage are measured using a standard voltage bridge. The signal is wirelessly transmitted to a base station for storage and processing. Breaths can be detected from the location of the peaks on a voltage–time graph; hence, the breathing rate can be deduced from the average time difference between successive peaks.

Along with a similar design concept, Guo et al. [95] integrated two conductive coated straps into a wearable vest, with the straps following the circumference of the chest and abdomen. The conductive coating is applied using the "knife-over-role" laboratory coating method. The control unit (consisting of a microcontroller and a Bluetooth transmitter) is situated on the back of the garment.

TABLE V
SUMMARY OF SKIN CONTACT WEARABLE SENSORS, SMART TEXTILES, AND WEARABLE VESTS USED TO MEASURE THE BREATHING RATE

| Lead author or product name | Description of sensor | Sensor placement on the body | Quantity being measured during respiration | Suitability for asthma monitoring | Clinically proven | Mobile Apps |
|---|---|---|---|---|---|---|
| Respira Sense [34] | Sensors made from piezoelectric films. | Attached directly to the skin using medical-grade adhesive. | The relative angle change between the thoracic and abdominal surfaces. | Low potential | Yes | Yes |
| M. Chu [91], [92] | Sensors made from a piezoelectric metal film using Shrinky Dink toys technology. | Attached directly to the skin around the circumference of the abdomen and ribcage using double-sided adhesive. | The change in strain. | Low potential | No | No |
| BioHarness 3.0 [93] | Capacitive pressure sensor. | Integrated into a wearable vest. | The change in torso circumference. | Medium potential | No | Yes |
| S. Brady [94] | Polypyrrole (conducting electroactive polymer) sensors. | Sewn into the pocket of a T-shirt. | The potential difference across the sensors (using a standard voltage bridge) due to. their varying compression. | Low potential | No | No |
| L. Guo [95] | Conductively coated straps act as sensors. | Integrated around the torso circumference in a wearable vest. | The changing resistance of the straps due to their varying compression. | Low potential | No | No |
| R. T. Brouillette [96] | Inductive bands act as sensors. | Integrated into a wearable vest. | The changing inductance of the bands. | Low potential | No | No |
| P.Y. Carry [97] | Two inductive coils act as sensors. | Integrated into a circumferential direction around the torso in a jacket. | The resistance as the coils due to their varying compression. | Low potential | No | No |
| A. Issatayeva [98] | Fibre Bragg Grating (FBG) sensors. | Two bands, each with five FBG sensors, are integrated into a wearable shirt around the chest and abdomen areas. | The wavelength of the reflected light. | Low potential | No | No |

Conductive threads are used to connect the straps to the control unit and are sewn into the piping of the garment along the seams. The resistive change due to the mechanical deformation of the sensor as the patient inhales and exhales is measured, from which the breathing rate can also be extracted.

Following a similar approach, Brouillette et al. [96] placed inductive bands around the chest, which changed inductance as the patient inhaled and exhaled during the respiratory cycle. The bands are then connected to a polygraph to give a signal trace, where the breathing rate can be extracted from the time difference between successive peaks identified after peak threshold detection was applied. The inductive plethysmography approach was also followed by Carry et al. [97], where two coils were integrated into a jacket and allowed only to move in the axial direction. This ensured that the changes in induction of the wires correspond to the movement of the chest during the respiration cycle.

Issatayeva et al. [98] created a different smart textile by mounting two belts (each with five sensors) onto a T-shirt, with the belts located around the abdomen and chest. The sensor used was a fiber Bragg grating (FBG) sensor. As light propagates through the sensor, a specific wavelength of light (the Bragg wavelength) is reflected. When an external strain or temperature acts upon the sensor, the reflected light shifts wavelength as the fibers within the sensor react. By measuring the wavelength of the reflected light, the strain (hence the change in circumference of the chest) can be found, from which breaths and the breathing rate can be extracted. As ten sensors are included within the garment, if six or more of the sensors show peaks simultaneously in their signal, these peaks are interpreted as corresponding to breaths and hence are used in the calculation of the breathing rate.

### *B. Monitoring Asthma Using Vital Signs Associated With Breathing Rate and Airflow Sound*

Table VI provides an overview of technologies used to measure other vital signs that are associated with the breathing rate and airflow sound and then discusses the suitability for use in people with asthma.

Fig. 5 shows the prototypes for a wearable patch and wristband. Sensors in both devices can track vital signs, including heart rate, respiratory rate, and oxygen saturation, provide estimations of wheezing in the lungs, and detect contamination in the air for patients with asthma [6].

Figs. 6 and 7 show chest motion sensors developed based on airflow sound. Fig. 8 shows a humidity sensor based on poly lactic glycolic acid.

A wheezing sensor can also be used to detect early indications of asthma. One such sensor with a breathing acquisition module can be placed on the upper chest to record the breathing sound. Once this signal has been wirelessly transmitted to an external device and processed, the signal can be displayed, and signs of wheezing can be identified. A commercially available and clinically approved wheezing sensor, Omron WheezeScan, is shown in Graphical Abstract (f).

Another type of asthma patient monitoring is achieved by measuring the concentration of nitric oxide, a chemical produced in response to airway inflammation caused by asthma [6]. Nitric oxide is not a vital sign measurement, but we believe that it is helpful to mention this technology to readers.

For people with asthma, a higher level of nitric oxide in their exhalation is related to the severity of airway inflammation. The nitric oxide of exhalation can be tested by handheld devices and used as a part of the patient monitoring scheme. Fig. 9 shows the devices used in primary care to measure the nitric oxide level and help in the early detection

TABLE VI
SUMMARY OF TECHNOLOGIES USED TO MEASURE OTHER VITAL SIGNS ASSOCIATED WITH THE BREATHING RATE AND AIRFLOW SOUND

| Lead author or product name | Vital sign | Sensor | Developed for asthma monitoring? | Suitability for asthma monitoring | Body contact type | Clinically proven? | Mobile Apps |
|---|---|---|---|---|---|---|---|
| Browne [103] | Airflow sound | PPG | No | High potential | Yes | Yes | Yes |
| HARS (Hybrid Aspiration and Respiration Sensing) [99] | Airflow sound | Chest motion sensor **(Fig. 6)** | Yes | Yes | Yes | No | No |
| Li [100] | Airflow sound | Chest motion sensor **(Fig. 7)** | No | Medium potential | Yes | No | No; has Bluetooth connection |
| Agnihotri [105] | Airflow temperature and respiration rate | Temperature sensor on the chest | No | Medium potential | Yes | No | No |
| Milici [106] | Apnoea during sleep | Temperature sensor on forehead and nose | No | Low potential | Yes | No | No |
| PEP (pyroelectric polymer) device [107] | Airflow CO2 | Pyroelectric polymer | No | Low potential | Yes | No | No |
| S. Xiao [108] | Humidity of airflow | Respiratory rate | No | Medium potential | Yes | No | No |
| S. Malik [109] | Humidity of airflow | Ionogel based | No | Low potential | Yes | No | No |
| A.M. Soomro [101] | Humidity of airflow | humidity sensor for respiratory rate | No | Low potential | Yes | No | No |
| A. Prochazka [110] | Airflow temperature | Capacitive sensor for respiratory rate Humidity sensor based on poly lactic glycolic acid **(Fig. 8)** | No | Medium potential | No | No | No |
| N. Andersen [111] | Chest movement | Infrared thermography Pulse-based radar system on chip for respiratory rate | No | Medium potential | No | No | No |
| Omron WheezeScan [112] | Airflow sound | Wheeze sensor **(Graphical Abstract f)** | Yes | Yes | Yes | Yes | Yes |

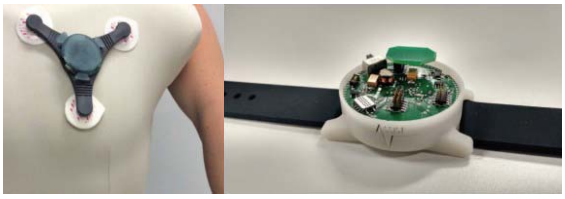

Fig. 5. Prototype for a chest patch and a wristband that can track vital signs and environmental factors [6].

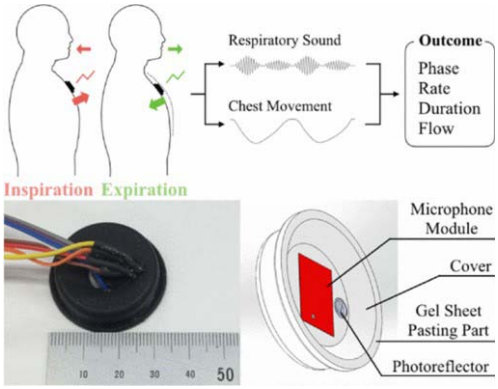


Fig. 6. Hybrid-based aspiration and respiration sensing for airflow sound [99].

of asthma attacks [102], [114]. Another monitor developed under a similar concept is a handheld asthma sensor with ZCube. This rechargeable sensor detects nitric oxide markers in exhales to help doctors adjust patients' medication dosage [13].

## V. DEVICES AND APPLICATIONS TRAILED FOR CLINICAL OBSERVATION AND INTERVENTIONS

People living with asthma require self-management, including observing breath patterns and enabling exercise control, as well as clinical intervention through medication intervention and treatment.

To provide insight into wearable and monitoring technologies used in clinical practices worldwide, we screened 248 studies using the keyword "monitoring" and 16 studies using the keyword "wearable" under the health condition of asthma on the NIH clinical trials database (accessed on July 28, 2022). This database is a major registration resource for privately and publicly funded clinical studies conducted worldwide, managed by the NIH U.S. National Library of Medicine.

After shortlisting clinical trials using keywords and removing clinical trials that were terminated, we shortlisted 11 clinical studies that focus on using wearable monitoring for asthma patient monitoring.

A key difference between clinical and nonclinical devices is the purpose of using them. For clinical studies, devices are used to obtain measurements to provide the detailed vital signs that are not necessarily needed in nonclinical settings. These measurements are called "outcome measures," as shown in Table VII. Researchers designing new vital signs monitoring technology for asthma monitoring should use clinical trial protocols such as the dictionary of "clinical importance," "ground-truth measurement," and "clinical or nonclinical pipeline." The types of vital signs used in clinical studies can be broader than the ones that are ready for commercially ready applications,

TABLE VII
SENSOR TECHNOLOGIES, OUTCOME MEASURES, PATIENT SIZE, COUNTRY OF USE, COMPLETION STATUS IN CLINICAL STUDIES, AND REVIEWER COMMENTS

| Study Title (Trial Period) | Enrollment (Age in Years) | Sponsor, Country | Outcome Measure | Vital Signs | Device Name and Sensor Technology | Mobile Apps |
|---|---|---|---|---|---|---|
| Automated Device for Asthma Monitoring (2009-2013) | 84 (13-17) | University of Rochester, US | Average Number of Coughs Per Hour | Cough | ADAM: Automated Device for Asthma Monitoring | N/A |
| Study of Monitoring Exhaled NO in Symptomatic Asthmatic Adults and Children During Anti-inflammatory Treatment (2006-2007) [114] | 151(4-65) | Aerocrine AB, Sweden | Percent change in FENO measured with NIOX MINO and NIOX between Visit 1 to Visit 2 | NO | The Aerocrine NIOX MINO Airway Inflammation Monitor | N/A |
| The Nature of Reflux-respiratory Symptoms Association in Difficult to Treat Wheezing Coughing Babies (2007-2011) | 15 (1-18 months) | Wolfson Medical Center, UK | | Wheezy sound | WEEM | N/A |
| Respiratory Disorders Non-invasive Monitoring of Work of Breathing in Outpatients (2020-2021) | 12 (18 and older) | Stanford University, Work of Breathing Study Group, US | Heart Rate and Respiratory rate | heart rate, respiratory rate | Contactless heart rate and respiratory rate monitor | N/A |
| Demonstration of Broncholytic Effects in Subjects With Obstructive Airway Diseases by Low Frequency Ultrasound (2010-2010) | 50 (18-70) | Fraunhofer-Institute of Toxicology and Experimental Medicine and Institute for Pharmacology and Toxicology, Germany | Change of the difference between expiratory and inspiratory TOF Expectation: a change above 10us will be considered significant | TOF | Low-frequency ultrasound spectroscopy after broncholysis | N/A |
| Research on the Early Warning Model of Children Asthma Acute Attack Based on Wearable Wrist Smart Device of Huami (2021-2024, estimated) | 200 | Guangzhou Institute of Respiratory Disease, China | Heart rate, blood oxygen, exercise, sleep, weight, height | Heart rate, blood oxygen | Huami wearable wrist Smart Device [115] | Yes |
| Safety and Feasibility of a Novel Device for Assessing Respiratory Function in Children (2021-2022) | 30 (3-18) | ResMed, US | Slow vital capacity from Leo device, PNT device | Respiratory rate | Leo device [116] | Yes |
| A Feasibility Study of SenseGuard to Assess Airway Responsiveness During Methacholine Challenge Test (2021-2022, estimated) | 40 (18 and older) | NanoVation, Canada | Respiratory parameters (Inhalation and Exhalation time and ratio) | Respiratory rate | SenseGuardTM [117] | N/A |
| Advanced Multimodal Wireless Vital Signs Monitoring for Patients With Asthma and Anaphylaxis (2021-2023, estimated) | 150 (1-17) | Northwestern University and Ann & Robert H Lurie Children's Hospital of Chicago, US | Percent agreement with pilot sensor and current standard | N/A | Advanced multimodal wireless vital signs monitor | N/A |
| Acoustic Cough Monitoring for the Management of Patients With Known Respiratory Disease (2021-2022, estimated) | 100 (5-100) | Clinica Universidad de Navarra, Universidad de Navarra,Centre de Recherche du Centre Hospitalier de l'Universit de Montral, and Hyfe, Inc, Spain | Correlation between subjective perception of cough and objective frequency, sensitivity and specificity of the system discriminating coughs | Cough | Hyfe Cough Tracker, Hyfe Air [118] | Yes |
| Loop Band Validation Study (2017-2018) | 235 (18 and older) | Spry Health, US | Device Equivalence in clinical outcome measures (heart rate, blood oxygenation, carboxyhemoglobin level, end tidal carbon dioxide, and respiratory rate) measured by Arterial Line. | pulse oximetry, respiration rate, and heart rate | Loop Band | N/A |

comparing Table VII to Table VI. To enable clinical usage, the clinical devices require a user interface to connect with a hospital IT system or the results need to be manually added to the electronic health record. The devices for clinical usage can be larger in size compared to home monitoring devices.

Table VII summarizes the shortlisted studies and lists their sensor technologies, name of devices, outcome measures, patient size, and country of use. These studies focus on technologies for asthma symptom monitoring and medical intervention. The clinical pipelines for observation and intervention are different when monitoring patients with asthma. The observation study will lead to a scientific conclusion based on observation, with or without medical intervention followed by.

Countries with different prevalence levels of asthma, limitations in doctor resources, or different income levels, such as low-and-medium-income countries, often require cost-effective and different digital health solutions to address their challenges. Country-specific information will help to

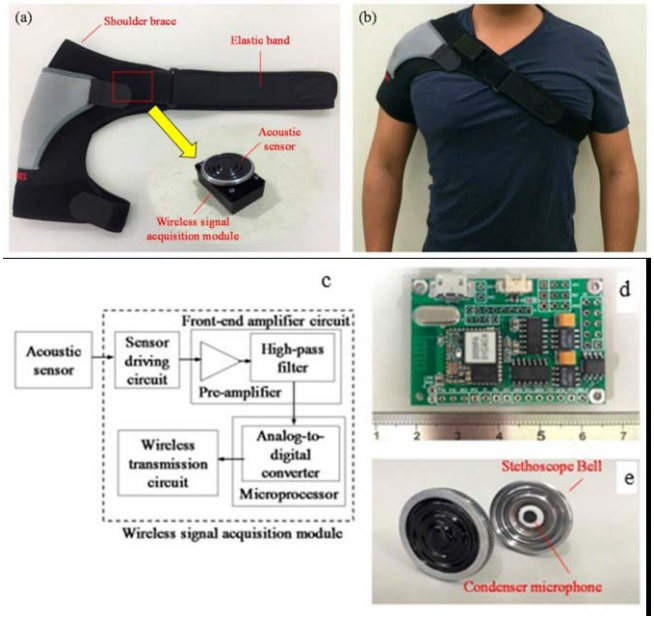


Fig. 7. Chest motion sensors. (a) Photograph of wearable mechanical design. (b) Photograph of wearing the wireless breathing sound monitoring system. (c) Block diagram and (d) photograph of the proposed wireless breathing sound acquisition module. (e) Photograph of the acoustic sensor [100].

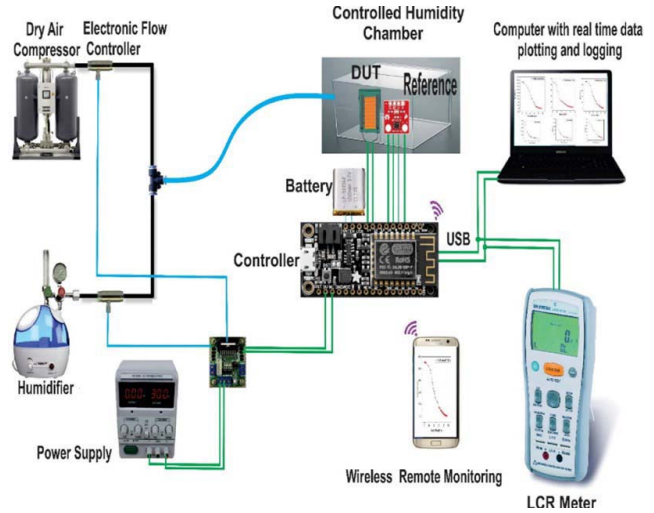


Fig. 8. Prototype of the breathing rate measurement using a humidity sensor based on poly lactic glycolic acid [101].

Fig. 9. Handheld nitric oxide devices. (a) NObreath FeNO primary care monitor for asthma monitoring [102]. (b) NIOX MINO for the monitoring of respiratory disorders [114].

address risk factors, diagnosis criteria in racial variance, and geographical differences that suit epidemiology studies. Readers interested in clinical trials can read the full details of the above trials on the NIH website [104].

## VI. Conclusion

This article has presented various methodologies in wearable vital sign monitoring for patients with asthma, including extracting breathing rate from ECG and PPG signals, monitoring airway sound in exhalation, and measuring breathing rate indirectly using a combination of wearable sensors and smart textiles. These sensor technologies' commercial and clinical applications and their readiness are summarized and discussed in Sections IV and V.

Although the direct measurement methods, such as the wearable vests and smart textile applications discussed in this article, provide the results that are strongly correlated with the breathing rate obtained from various clinical "gold-standard" techniques, there are some common challenges in long-term breathing rate monitoring for patients with asthma.

First, the conditions in which the different sensors were tested do not accurately reflect the environment in which they will be used. There will be significantly more motion artifacts present outside of clinical trials as the patient follows their normal daily routine; thus, the processing techniques used for extracting the breathing rate from the signal will not necessarily yield the same accuracy of results.

Second, some sensor monitoring technologies require specialized garments to be worn by the patient. As the patient would also need to be continuously monitored, they would either need to wash the garments regularly or own multiple garments—with these solutions being either impractical or expensive.

In addition, when the garments are not discreet but instead are vests and T-shirts that need to be tight-fitting to ensure good contact between the sensors and the chest, it is unlikely that patients will be willing to wear these garments every day instead of their own clothing. Therefore, these methods do not present desirable means for continuous monitoring of the breathing rate in asthmatic patients.

Extracting breathing rate from ECG and PPG signals provides a more realistic opportunity for continuous monitoring, as recording these signals can be achieved using smaller, integrated sensors that have minimal impact on the patient's day-to-day life. For example, as a lot of patients wear rings daily, the Oura ring is small, compact, and minimally affects the patient. Moreover, with the ever-increasing use of smartphones and smart watches, applications with smartphone and watches can also be feasible solutions for long-term asthma monitoring.

Furthermore, as there are a large variety of techniques to extract the breathing rate from the signals, a combination of the algorithms could potentially be used to ensure a more accurate calculation of the breathing rate.

In conclusion, continuous monitoring of patients' breathing rate and airflow sound would enable periods of patient decline to be more quickly identified, allowing more timely intervention for medical treatment and potentially preventing the patient from requiring admission to

the emergency department. Asthma monitoring can improve patient's quality of life, potentially reduce hospital admissions, and serve cases, thus preventing some deaths, thus beneficial to both the National Health Service and individuals affected by asthma.

## Acknowledgment

David Clifton is an Investigator at the Pandemic Sciences Institute, University of Oxford, Oxford, U.K. The views expressed are those of the authors and not necessarily those of the NHS, the NIHR, the Department of Health, the University of Oxford, or InnoHK–ITC.

## References

[1] WHO. *Asthma*. Accessed: May 6, 2022. [Online]. Available: https://www.who.int/news-room/fact-sheets/detail/asthma

[2] National Institute for Health and Care Excellence. *What Is the Prevalence of Asthma*. Accessed: May 6, 2022, [Online]. Available: https://cks.nice.org.uk/topics/asthma/background-information/prevalence/

[3] M. Masoli, D. Fabian, S. Holt, and R. Beasley, "The global burden of asthma: Executive summary of the GINA dissemination committee report," *Allergy*, vol. 59, no. 5, pp. 469–478, May 2004, doi: 10.1111/j.1398-9995.2004.00526.x.

[4] Asthma Lung UK. *What Is Asthma*. Accessed: Apr. 5, 2022. [Online]. Available: https://www.asthma.org.uk/advice/understanding-asthma/what-is-asthma/

[5] S. Papiris, A. Kotanidou, K. Malagari, and C. Roussos, "Clinical review: Severe asthma," *Crit. Care*, vol. 6, no. 1, pp. 30–44, Feb. 2002, doi: 10.1186/cc1451.

[6] W. Yan, "Toward better management for asthma: From smart inhalers to injections to wearables, researchers are finding new ways to improve asthma treatment," *IEEE Pulse*, vol. 9, no. 1, pp. 28–33, Jan. 2018, doi: 10.1109/mpul.2017.2772398.

[7] X. Ding et al., "Wearable sensing and telehealth technology with potential applications in the coronavirus pandemic" *IEEE Rev. Biomed. Eng.*, vol. 14, pp. 48–70, 2021, doi: 10.1109/RBME.2020.2992838.

[8] N. Ji et al., "Potential applications of wearable sensors in closed-loop management of STEMI patients during pandemics," Presented at the 42nd Annu. Int. Conf. IEEE Eng. Med. Biol. Soc., Montreal, QC, Canada, Jul. 2020.

[9] X. Wang, Q. Gui, B. Liu, Z. Jin, and Y. Chen, "Enabling smart personalized healthcare: A hybrid mobile-cloud approach for ECG telemonitoring," *IEEE J. Biomed. Health Informat.*, vol. 18, no. 3, pp. 739–745, May 2014.

[10] (2012). *IEEE Life Sciences Grand Challenges Conference*. [Online]. Available: https://lifesciences.ieee.org/lsgcc/2012-ieee-life-sciences-grandchallenges-conference/

[11] Asthma UK. *What Is Asthma?* Accessed: Jul. 10, 2021. [Online]. Available: https://www.asthma.org.uk/advice/understanding-asthma/what-is-asthma/

[12] Asthma UK. *Asthma Triggers*. Accessed: Jul. 10, 2021. [Online]. Available: https://www.asthma.org.uk/advice/triggers/

[13] H. Knight, "Breath sensor can predict an asthma attack the day before," *New Sci.*, vol. 209, no. 2798, p. 22, Feb. 2011.

[14] C. Walker, S. Gupta, R. Hartley, and C. E. Brightling, "Computed tomography scans in severe asthma: Utility and clinical implications," *Current Opinion Pulmonary Med.*, vol. 18, no. 1, pp. 42–47, Jan. 2012, doi: 10.1097/MCP.0b013e32834db255.

[15] P. Haldar et al., "Mepolizumab and exacerbations of refractory eosinophilic asthma," *New England J. Med.*, vol. 360, no. 10, pp. 973–984, Mar. 2009, doi: 10.1056/NEJMoa0808991.

[16] K. Kasahara, K. Shiba, T. Ozawa, K. Okuda, and M. Adachi, "Correlation between the bronchial subepithelial layer and whole airway wall thickness in patients with asthma," *Thorax*, vol. 57, no. 3, pp. 242–246, Mar. 2002, doi: 10.1136/thorax.57.3.242.

[17] A. Niimi et al., "Airway wall thickness in asthma assessed by computed tomography: Relation to clinical indices," *Amer. J. Respiratory Crit. Care Med.*, vol. 162, no. 4, pp. 1518–1523, Oct. 2000, doi: 10.1164/ajrccm.162.4.9909044.

[18] J. de Blic, I. Tillie-Leblond, S. Emond, B. Mahut, T. L. Dang Duy, and P. Scheinmann, "High-resolution computed tomography scan and airway remodeling in children with severe asthma," *J. Allergy Clin. Immunol.*, vol. 116, no. 4, pp. 750–754, Oct. 2005, doi: 10.1016/j.jaci.2005.07.009.

[19] S. Saglani et al., "Can HRCT be used as a marker of airway remodelling in children with difficult asthma?" *Respiratory Res.*, vol. 7, no. 1, p. 46, Mar. 2006, doi: 10.1186/1465-9921-7-46.

[20] G. Luo et al., "Predicting asthma control deterioration in children," *BMC Med. Informat. Decis. Making*, vol. 15, no. 1, p. 84, Oct. 2015, doi: 10.1186/s12911-015-0208-9.

[21] British Lung Foundation. *SaniQ Asthma—Pollen and Asthma*. Accessed: Jul. 4, 2021. [Online]. Available: https://www.blf.org.uk/technology-for-lung-health/saniq-asthma-pollen-asthma

[22] Propeller Health. *Meet Propeller. The Doctor-Recommended Way to Manage Your Asthma or COPD*. Accessed: Aug. 6, 2021. [Online]. Available: https://propellerhealth.com/.

[23] Smart Asthma. *Asthma Control in Your Pocket*. Accessed: Aug. 5, 2021. [Online]. Available: https://smartasthma.com/

[24] D. Moran and L. Mendal, "Core temperature measurement," *Sports Med.*, vol. 32, pp. 879–885, Oct. 2002, doi: 10.2165/00007256-200232140-00001.

[25] University of Rochester Medical Centre. *Vital Signs (Body Temperature, Pulse Rate, Respiration Rate, Blood Pressure)*. Accessed: Jul. 3, 2021. [Online]. Available: https://www.urmc.rochester.edu/encyclopedia/content.aspx?

[26] D. Jones, L. Appel, and S. Sheps, "Measuring blood pressure accurately: New and persistent challenges," *J. Amer. Med. Assoc.*, vol. 289, no. 8, pp. 1027–1030, Feb. 2003, doi: 10.1001/jama.289.8.1027.

[27] M. Sinha and C. Reid, "Systemic hypertension," in *Paediatric Cardiology*, 3rd ed. Philadelphia, PA, USA: Churchill Livingstone, 2010, ch. 58, pp. 1191–1217.

[28] A. Plüddemann, M. Thompson, C. Heneghan, and C. Price, "Pulse oximetry in primary care: Primary care diagnostic technology update," *Brit. J. Gen. Pract.*, vol. 61, no. 586, pp. 358–359, May 2011, doi: 10.3399/bjgp11X572553.

[29] V. Kamat, "Pulse oximetry," *Indian J. Anaesthesia*, vol. 46, no. 4, pp. 261–268, Aug. 2002.

[30] British Lung Foundation. *Breathing and Lung Function Tests*. Accessed: Jul. 2, 2021. [Online]. Available: https://www.blf.org.uk/support-for-you/breathing-tests/tests-measure-oxygen-levels

[31] K. Khunti, "Accurate interpretation of the 12-lead ECG electrode placement: A systematic review," *Health Educ. J.*, vol. 73, no. 5, pp. 610–623, Apr. 2013, doi: 10.1177/0017896912472328.

[32] C.-C. Hsu, B.-S. Lin, K.-Y. He, and B.-S. Lin, "Design of a wearable 12-lead noncontact electrocardiogram monitoring system," *Sensors*, vol. 19, no. 7, p. 1509, Mar. 2019, doi: 10.3390/s19071509.

[33] NHS. *Electrocardiogram (ECG)*. Accessed: Aug. 10, 2021. [Online]. Available: https://www.nhs.uk/conditions/electrocardiogram/

[34] C. Subbe and S. Kinsella, "Continuous monitoring of respiratory rate in emergency admissions: Evaluation of the RespiraSense sensor in acute care compared to the industry standard and gold standard," *Sensors*, vol. 18, no. 8, p. 2700, Aug. 2018, doi: 10.3390/s18082700.

[35] J. Gravenstein, M. Jaffe, N. Gravenstein, and D. Paulus, "Clinical perspectives," in *Capnography*, 2nd ed. Cambridge, U.K.: Cambridge Univ. Press, 2011, ch. 1, pp. 1–8.

[36] N. Nayan, N. Risman, and R. Jaafar, "Breathing rate estimation from a single-lead electrocardiogram acquisition system," *Int. J. Appl. Eng. Res.*, vol. 10, no. 17, pp. 38154–38158, Jan. 2015.

[37] E. Helfenbein, R. Firoozabadi, S. Chien, E. Carlson, and S. Babaeizadeh, "Development of three methods for extracting respiration from the surface ECG: A review," *J. Electrocardiol.*, vol. 47, no. 6, pp. 819–825, Nov. 2014, doi: 10.1016/j.jelectrocard.2014.07.020.

[38] R. Ruangsuwana, G. Velikic, and M. Bocko, "Methods to extract respiration information from ECG signals," in *Proc. ICASSP*, Dallas, TX, USA, 2010, pp. 570–573.

[39] Y. Wang, C. J. Deepu, and Y. Lian, "A computationally efficient QRS detection algorithm for wearable ECG sensors," in *Proc. IEEE EMBC*, Boston, MA, USA, Aug. 2011, pp. 5641–5644.

[40] X. Tang, Q. Hu, and W. Tang, "A real-time QRS detection system with PR/RT interval and ST segment measurements for wearable ECG sensors using parallel delta modulators," *IEEE Trans. Biomed. Circuits Syst.*, vol. 12, no. 4, pp. 751–761, Aug. 2018, doi: 10.1109/TBCAS.2018.2823275.

[41] N. Ravanshad, H. Rezaee-Dehsorkh, R. Lotfi, and Y. Lian, "A level-crossing based QRS-detection algorithm for wearable ECG sensors," *IEEE J. Biomed. Health Informat.*, vol. 18, no. 1, pp. 183–192, Jan. 2014, doi: 10.1109/JBHI.2013.2274809.

[42] X. Zhang and Y. Lian, "A 300-mV 220-nW event-driven ADC with real-time QRS detection for wearable ECG sensors," *IEEE Trans. Biomed. Circuits Syst.*, vol. 8, no. 6, pp. 834–843, Dec. 2014, doi: 10.1109/TBCAS.2013.2296942.

[43] K. Zhao, Y. Li, G. Wang, Y. Pu, and Y. Lian, "A robust QRS detection and accurate R-peak identification algorithm for wearable ECG sensors," *Sci. China Inf. Sci.*, vol. 64, no. 8, pp. 1–17, May 2021, doi: 10.1007/S11432-020-3150-2.

[44] C. O'Brien and C. Heneghan, "A comparison of algorithms for estimation of a respiratory signal from the surface electrocardiogram," *Comput. Biol. Med.*, vol. 37, no. 3, pp. 305–314, Mar. 2007, doi: 10.1016/j.compbiomed.2006.02.002.

[45] A. Fusco, D. Locatelli, F. Onorati, G. C. Durelli, and M. D. Santambrogio, "On how to extract breathing rate from PPG signal using wearable devices," in *Proc. BioCAS*, Atlanta, GA, USA, Oct. 2015, pp. 1–4.

[46] M. Ambekar and S. Prabhu, "A novel algorithm to obtain respiratory rate from the PPG signal," *Int. J. Comput. Appl.*, vol. 126, no. 15, pp. 9–12, Sep. 2015, doi: 10.5120/ijca2015906263.

[47] D. Li, H. Zhao, and S. Dou, "A new signal decomposition to estimate breathing rate and heart rate from photoplethysmography signal," *Biomed. Signal Process. Control*, vol. 19, pp. 89–95, May 2015, doi: 10.1016/j.bspc.2015.03.008.

[48] S. Fleming and L. Tarassenko, "A comparison of signal processing techniques for the extraction of breathing rate from the photoplethysmogram," *Int. J. Biol. Med. Sci.*, vol. 2, no. 4, pp. 232–236, Jan. 2007. [Online]. Available: https://www.researchgate.net/publication/228907148

[49] L. Nilsson, T. Goscinski, A. Johansson, L.-G. Lindberg, and S. Kalman, "Age and gender do not influence the ability to detect respiration by photoplethysmography," *J. Clin. Monit. Comput.*, vol. 20, no. 6, pp. 431–436, Oct. 2006.

[50] P. Leonard, T. F. Beattie, P. S. Addison, and J. N. Watson, "Standard pulse oximeters can be used to monitor respiratory rate," *Emergency Med. J.*, vol. 20, no. 6, pp. 524–525, Nov. 2003, doi: 10.1136/emj.20.6.524.

[51] Physics World. *Low-Cost Wearable Devices Quantify Breathing Activity While You Sleep*. Accessed: Jun. 30, 2021. [Online]. Available: https://physicsworld.com/a/low-cost-wearable-devices-quantify-breathing-activity-while-you-sleep/

[52] Z. Zhang, W. Wang, B. Wang, H. Wu, H. Liu, and Y. Zhang, "A prototype of wearable respiration biofeedback platform and its preliminary evaluation on cardiovascular variability," in *Proc. 3rd Int. Conf. Bioinf. Biomed. Eng.*, Bejing, China, Jun. 2009, pp. 1–4.

[53] C. Park, P. H. Chou, Y. Bai, R. Matthews, and A. Hibbs, "An ultra-wearable, wireless, low power ECG monitoring system," in *Proc. IEEE BioCAS*, London, U.K., Nov. 2006, pp. 241–244.

[54] R. Fensli, E. Gunnarson, and T. Gundersen, "A wearable ECG-recording system for continuous arrhythmia monitoring in a wireless tele-home-care situation," in *Proc. CBMS*, Dublin, Ireland, 2005, pp. 407–412.

[55] D. Yamamoto, S. Nakata, K. Kanao, T. Arie, S. Akita, and K. Takei, "All-printed, planar-type multi-functional wearable flexible patch integrated with acceleration, temperature, and ECG sensors," in *Proc. MEMS*, Las Vegas, NV, USA, Jan. 2017, pp. 239–242.

[56] Y. Yamamoto et al., "Efficient skin temperature sensor and stable gel-less sticky ECG sensor for a wearable flexible healthcare patch," *Adv. Healthcare Mater.*, vol. 6, no. 17, Jun. 2017, Art. no. 1700495, doi: 10.1002/ADHM.201700495.

[57] Apple. *ECG App and Irregular Heart Rhythm Notification Available Today on Apple Watch*. Accessed: Mar. 29, 2022. [Online]. Available: https://www.apple.com/uk/newsroom/2019/03/ecg-app-and-irregular-rhythm-notification-on-apple-watch-available-today-across-europe-and-hong-kong/

[58] Withings. *Record an ECG Anytime, Anywhere*. Accessed: Mar. 29, 2022. [Online]. Available: https://www.withings.com/uk/en/move-ecg

[59] N. G. Hallfors et al., "Graphene oxide: Nylon ECG sensors for wearable IoT healthcare—Nanomaterial and SoC interface," *Anal. Integr. Circuits Signal Process.*, vol. 96, no. 2, pp. 253–260, Feb. 2018, doi: 10.1007/s10470-018-1116-6.

[60] E. Nemati, M. J. Deen, and T. Mondal, "A wireless wearable ECG sensor for long-term applications," *IEEE Commun. Mag.*, vol. 50, no. 1, pp. 36–43, Jan. 2012, doi: 10.1109/MCOM.2012.6122530.

[61] E. Sardini and M. Serpelloni, "Instrumented wearable belt for wireless health monitoring," in *Proc. Eurosensors XXIV*, Linz, Austria, 2010, pp. 580–583.

[62] O. Banos, C. Villalonga, M. Damas, P. Gloesekoetter, H. Pomares, and I. Rojas, "PhysioDroid: Combining wearable health sensors and mobile devices for a ubiquitous, continuous, and personal monitoring," *Sci. World J.*, vol. 2014, Sep. 2014, Art. no. 490824, doi: 10.1155/2014/490824.

[63] A. A. Akintola, V. van de Pol, D. Bimmel, A. C. Maan, and D. van Heemst, "Comparative analysis of the equivital EQ02 lifemonitor with Holter ambulatory ECG device for continuous measurement of ECG, heart rate, and heart rate variability: A validation study for precision and accuracy," *Frontiers Physiol.*, vol. 7, Sep. 2016, Art. no. 391, doi: 10.3389/fphys.2016.00391.

[64] Equivital. *EQ Life Monitor*. Accessed: Jul. 22, 2021. [Online]. Available: https://www.equivital.com/products/eq02-lifemonitor?cn-reloaded=1

[65] P. Pandian et al., "Smart Vest: Wearable multi-parameter remote physiological monitoring system," *Med. Eng. Phys.*, vol. 30, no. 4, pp. 466–477, May 2008, doi: 10.1016/j.medengphy.2007.05.014.

[66] M. K. Yapici and T. E. Alkhidir, "Intelligent medical garments with graphene-functionalized smart-cloth ECG sensors," *Sensors*, vol. 17, no. 4, p. 875, Apr. 2017, doi: 10.3390/s17040875.

[67] Masimo. *Radius PPG Tetherless Pulse Oximetry*. Accessed: Mar. 29, 2022. [Online]. Available: https://www.masimo.com/products/sensors/radius-ppg/

[68] Fitbit. *Products*. Accessed: Mar. 29, 2022. [Online]. Available: https://www.fitbit.com/global/uk/products/trackers/

[69] Biobeat. *Wrist Monitor*. Accessed: Mar. 29, 2022. [Online]. Available: https://www.bio-beat.com/products

[70] M. Ringwald, A. Crich, and N. Beysard, "Smart watch recording of ventricular tachycardia: Case study," *Amer. J. Emergency Med.*, vol. 38, no. 4, p. 849, Apr. 2020, doi: 10.1016/j.ajem.2019.10.040.

[71] Apple. *Take an ECG With the ECG App on Apple Watch*. Accessed: Jul. 1, 2021. [Online]. Available: https://support.apple.com/en-us/HT208955know

[72] Withings. *Record an ECG Anytime, Anywhere*. Accessed: Jun. 29, 2021. [Online]. Available: https://www.withings.com/uk/en/move-ecg

[73] Kardia. *Kardia by AliveCor*. Accessed: Aug. 10, 2021. [Online]. Available: https://www.kardia.com/kardiamobile

[74] L. Koltowski et al., "Kardia mobile applicability in clinical practice: A comparison of Kardia mobile and standard 12-lead electrocardiogram records in 100 consecutive patients of a tertiary cardiovascular care center," *Cardiol. J.*, vol. 28, no. 4, pp. 543–548, Jul. 2021, doi: 10.5603/CJ.a2019.0001.

[75] Oura. *Products*. Accessed: Mar. 29, 2022. [Online]. Available: https://ouraring.com/product/

[76] A. Plüddemann, M. Thompson, C. Heneghan, and C. Price, "Pulse oximetry in primary care: Primary care diagnostic technology update," *Brit. J. Gen. Pract.*, vol. 61, no. 586, pp. 358–359, May 2011, doi: 10.3399/bjgp11X572553.

[77] W. S. Johnston and Y. Mendelson, "Extracting breathing rate information from a wearable reflectance pulse oximeter sensor," in *Proc. IEEE EMBS*, San Francisco, CA, USA, Sep. 2004, pp. 5388–5391.

[78] BXS Insight. *BSX Insight Endurance Evolved*. Accessed: Aug. 10, 2022. [Online]. Available: https://www.bsxinsight.com

[79] Homon. *Humon Muscle Oxygen Sensor*. Accessed: Aug. 10, 2022. [Online]. Available: https://www.humon.io

[80] O. Chetélat et al., "Clinical validation of LTMS-S: A wearable system for vital signs monitoring," in *Proc. 37th Annu. Int. Conf. IEEE Eng. Med. Biol. Soc. (EMBC)*, Piscataway, NJ, USA, Aug. 2015, pp. 3125–3128.

[81] Oura. *Ring and App*. Accessed: Aug. 20, 2021. [Online]. Available: https://ouraring.com/blog/the-oura-difference/

[82] Medical Product Outsourcing. *FDA Clears Masimo's Radius PPG, the First Tetherless SET Pulse Oximetry Sensor Solution*. Accessed: Jul. 15, 2021. [Online]. Available: https://www.mpo-mag.com/contents/viewbreaking-news/2019-05-16/fda-clears-masimos-radius-ppg-the-first-etherless-set-pulse-oximetry-sensor-solution/

[83] *Lumafit*. Accessed: Aug. 18, 2022. [Online]. Available: https://www.lumafit.com

[84] Biobeats. *Wrist Monitor*. Accessed: Jul. 27, 2021. [Online]. Available: https://www.bio-beat.com/copy-of-clinical-trials-and-researc-1

[85] Y. Bai, P. Hibbing, C. Mantis, and G. J. Welk, "Comparative evaluation of heart rate-based monitors: Apple watch vs fitbit charge HR," *J. Sports Sci.*, vol. 36, no. 15, pp. 1734–1741, Dec. 2017, doi: 10.1080/02640414.2017.1412235.
[86] A. Gorny, S. Liew, C. Tan, and F. Muüller-Riemenschneider, "Fitbit charge HR wireless heart rate monitor: Validation study conducted under free-living conditions," *JMIR Mhealth Uhealth*, vol. 5, no. 10, p. 157, Oct. 2017, doi: 10.2196/mhealth.8233.
[87] S. Benedetto, C. Caldato, E. Bazzan, D. Greenwood, V. Pensabene, and P. Actis, "Assessment of the fitbit charge 2 for monitoring heart rate," *PLoS ONE*, vol. 13, no. 2, Feb. 2018, Art. no. 192691, doi: 10.1371/journal.pone.01926911.
[88] Y. Lee, H. Shin, J. Jo, and Y.-K. Lee, "Development of a wristwatch-type PPG array sensor module," in *Proc. ICCE*, Berlin, Germany, Sep. 2011, pp. 168–171.
[89] S. H. Browne et al., "Smartphone biosensor with app meets FDA/ISO standards for clinical pulse oximetry and can be reliably used by a wide range of patients," *Chest*, vol. 159, no. 2, pp. 724–732, Feb. 2021, doi: 10.1016/j.chest.2020.08.2104.
[90] Bioharness. *Lightweight, Portable Data Logger and Telemetry System*. Accessed: Mar. 29, 2022. [Online]. Available: https://www.biopac.com/product/bioharness-telemetry-logging-systems/
[91] M. Chu et al., "Respiration rate and volume measurements using wearable strain sensors," *NPJ Digit. Med.*, vol. 2, no. 1, pp. 1–9, Feb. 2019, doi: 10.1038/s41746-019-0083-3.
[92] MedGadget. *Wearable Respiration Sensors Made From Shrinky Drinks*. Accessed: Aug. 8, 2021. [Online]. Available: https://www.medgadget.com/2019/02/wearable-respiration-sensors-made-from-shrinky-dinks.html
[93] S. Casaccia, F. Pietroni, A. Calvaresi, G. M. Revel, and L. Scalise, "Smart monitoring of user's health at home: Performance evaluation and signal processing of a wearable sensor for the measurement of heart rate and breathing rate," in *Proc. BIOSTEC*, Rome, Italy, 2016, pp. 175–182.
[94] S. Brady, D. Diamond, B. Carson, D. O'Gorman, and N. Moyna, "Combining wireless with wearable technology for the development of on-body networks," in *Proc. BSN*, Cambridge, MA, USA, 2006, p. 36.
[95] L. Guo, L. Berglin, Y. J. Li, H. Mattila, A. K. Mehrjerdi, and M. Skrifvars, "'Disappearing sensor'-textile based sensor for monitoring breathing," in *Proc. CASE*, Singapore, Jul. 2011, pp. 1–4.
[96] R. T. Brouillette, A. S. Morrow, D. E. Weese-Mayer, and C. E. Hunt, "Comparison of respiratory inductive plethysmography and thoracic impedance for apnea monitoring," *J. Pediatrics*, vol. 111, no. 3, pp. 377–383, Sep. 1987, doi: 10.1016/S0022-3476(87)80457-2.
[97] P.-Y. Carry, P. Baconnier, A. Eberhard, P. Cotte, and G. Benchetrit, "Evaluation of respiratory inductive plethysmography," *Chest*, vol. 111, no. 4, pp. 910–915, Apr. 1997, doi: 10.1378/chest.111.4.910.
[98] A. Issatayeva, A. Beisenova, D. Tosi, and C. Molardi, "Fiber-optic based smart textiles for real-time monitoring of breathing rate," *Sensors*, vol. 20, no. 12, p. 3408, Jun. 2020, doi: 10.3390/s20123408.
[99] Y. Yuasa, K. Takahashi, and K. Suzuki, "Wearable flexible device for respiratory phase measurement based on sound and chest movement," in *Proc. IEEE Int. Conf. Syst., Man, Cybern. (SMC)*, Oct. 2017, pp. 2378–2383, doi: 10.1109/SMC.2017.8122978.
[100] S.-H. Li, B.-S. Lin, C.-H. Tsai, C.-T. Yang, and B.-S. Lin, "Design of wearable breathing sound monitoring system for real-time wheeze detection," *Sensors*, vol. 17, no. 12, p. 171, Jan. 2017, doi: 10.3390/s17010171.
[101] A. M. Soomro, F. Jabbar, M. Ali, J.-W. Lee, S. W. Mun, and K. H. Choi, "All-range flexible and biocompatible humidity sensor based on poly lactic glycolic acid (PLGA) and its application in human breathing for wearable health monitoring," *J. Mater. Sci., Mater. Electron.*, vol. 30, no. 10, pp. 9455–9465, May 2019.
[102] NOBreath. *NObreath: The Primary Care FeNO Monitor*. Accessed: Aug. 28, 2022. [Online]. Available: https://www.nobreath.co.uk/nobreath-feno-monitor/
[103] T. Elfaramawy, C. L. Fall, S. Arab, M. Morissette, F. Lellouche, and B. Gosselin, "A wireless respiratory monitoring system using a wearable patch sensor network," *IEEE Sensors J.*, vol. 19, no. 2, pp. 650–657, Jan. 2019, doi: 10.1109/JSEN.2018.2877617.
[104] *US National Library of Medicine Clinical Trial Database*. Accessed: Aug. 25, 2022. [Online]. Available: https://clinicalTrials.gov
[105] A. Agnihotri, "Human body respiration measurement using digital temperature sensor with I2C interface," *Int. J. Sci. Res. Publications*, vol. 3, no. 3, pp. 232–238, 2013.
[106] S. Milici, J. Lorenzo, A. Lázaro, R. Villarino, and D. Girbau, "Wireless breathing sensor based on wearable modulated frequency selective surface," *IEEE Sensors J.*, vol. 17, no. 5, pp. 1285–1292, Mar. 2017, doi: 10.1109/JSEN.2016.2645766.
[107] C. N. Brookes, J. D. Whittaker, C. Moulton, and D. Dodds, "The PEP respiratory monitor: A validation study," *Emerg. Med. J.*, vol. 20, no. 4, pp. 326–328, Jul. 2003, doi: 10.1136/emj.20.4.326.
[108] S. Xiao et al., "Fast-response ionogel humidity sensor for real-time monitoring of breathing rate," *Mater. Chem. Frontiers*, vol. 3, no. 3, pp. 484–491, Feb. 2019, doi: 10.1039/C8QM00596F.
[109] S. Malik, M. Ahmad, M. Punjiya, A. Sadeqi, M. S. Baghini, and S. Sonkusale, "Respiration monitoring using a flexible paper-based capacitive sensor," in *Proc. IEEE SENSORS*, Oct. 2018, pp. 1–4, doi: 10.1109/ICSENS.2018.8589558.
[110] A. Procházka, H. Charvátová, O. Vyšata, J. Kopal, and J. Chambers, "Breathing analysis using thermal and depth imaging camera video records," *Sensors*, vol. 17, no. 6, p. 1408, Jun. 2017, doi: 10.3390/s17061408.
[111] N. Andersen et al., "A 118-mW pulse-based radar SoC in 55-nm CMOS for non-contact human vital signs detection," *IEEE J. Solid-State Circuits*, vol. 52, no. 12, pp. 3421–3433, Dec. 2017.
[112] S. Dramburg, E. Dellbrügger, W. van Aalderen, and P. M. Matricardi, "The impact of a digital wheeze detector on parental disease management of pre-school children suffering from wheezing—A pilot study," *Pilot Feasibility Stud.*, vol. 7, no. 1, pp. 1–10, Dec. 2021, doi: 10.1186/s40814-021-00917-w.
[113] S.-H. Li, B.-S. Lin, C.-H. Tsai, C.-T. Yang, and B.-S. Lin, "Design of wearable breathing sound monitoring system for real-time wheeze detection," *Sensors*, vol. 17, no. 12, p. 171, Jan. 2017, doi: 10.3390/s17010171.
[114] M. Maniscalco and J. O Lundberg, "Hand-held nitric oxide sensor NIOX MINO for the monitoring of respiratory disorders," *Expert Rev. Respiratory Med.*, vol. 4, no. 6, pp. 715–721, 2010, doi: 10.1586/ers.10.67.
[115] *Huami*. Accessed: Nov. 7, 2022. [Online]. Available: https://www.amazfit.com/en/watch-classify
[116] Leo. *Complete Asthma Management*. Accessed: Nov. 7, 2022. [Online]. Available: https://www.asthmaplatform.com/
[117] EU Horizon2020 Cordis. *A Breakthrough Respiratory Monitoring Device Incorporating Novel Nanotechnology-Based Sensors*. Accessed: Nov. 7, 2022. [Online]. Available: https://cordis.europa.eu/project/id/946598
[118] Hefe. *Track Your Cough*. Accessed: Nov. 7, 2022. [Online]. Available: https://www.hyfeapp.com/

**Lucy Taylor** received the M.Eng. degree from the Department of Engineering Science, University of Oxford, Oxford, U.K., in 2021.

She received the Somerville College Scholarship to work as an Intern at the Computational Health Informatics Laboratory, University of Oxford. Her research interest focuses on wearable devices and sensor technologies.

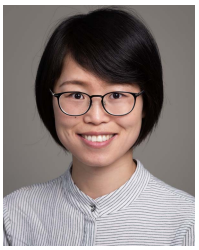

**Xiaorong Ding** (Member, IEEE) received the Ph.D. degree in biomedical engineering from the Department of Electronic Engineering, The Chinese University of Hong Kong (CUHK), Hong Kong, in 2016.

Before she joined University of Electronic Science and Technology of China (UESTC), Chengdu, China, in 2020, she did postdoctoral research at CUHK for one year and then at the University of Oxford, Oxford, U.K., for three years, with research work on developing intelligent systems that can monitor patient condition at home and help patients manage long-term conditions. She is currently a Research Associate Professor with the School of Life Science and Technology, UESTC. Her research interests lie in wearable health monitoring, biomedical signal processing, and smart healthcare.

**David Clifton** studied information engineering at the Department of Engineering Science, University of Oxford, Oxford, U.K., supervised by Prof. Lionel Tarassenko, CBE.

He is currently a Professor of Clinical Machine Learning and leads the Computational Health Informatics (CHI) Laboratory, also with the Oxford Suzhou Centre for Advanced Research is a sublaboratory of the CHI laboratory, Suzhou, China. He is also the Visiting Chair in AI for Health at The University of Manchester, Manchester, U.K., and a Fellow of Fudan University, Shanghai, China. He is an OCC Fellow of the AI and ML at Reuben College, a Research Fellow of the Royal Academy of Engineering, and a Fellow of the Alan Turing Institute. His research focuses on artificial intelligence (AI) for healthcare.

Prof. Clifton is an OCC Fellow of the AI and ML at Reuben College, a Research Fellow of the Royal Academy of Engineering, and a Fellow of the Alan Turing Institute. His research has won over 35 awards; he is a Grand Challenge awardee from the U.K. Engineering and Physical Sciences Research Council, which is an EPSRC Fellowship that provides long-term strategic support for nine "future leaders in healthcare." He was the joint winner of the inaugural "Vice-Chancellor's Innovation Prize," which identifies the best interdisciplinary research across the entirety of the University of Oxford.

**Huiqi Lu** (Member, IEEE) received the D.Phil. degree in industrial informatics and signal processing from the University of Sussex, Brighton, U.K., in 2008.

She is a Royal Academy of Engineering Daphne Jackson Research Fellow working at the Computational Health Informatics Laboratory, Institute of Biomedical Engineering, Department of Engineering Science, University of Oxford, Oxford, U.K. Her research focuses on artificial intelligence (AI) in healthcare, signal processing, and mathematical modeling.

Dr. Lu is also a Fellow of the Higher Education Academy, a Fulford Junior Research Fellow and a Governing Body Member of the Somerville College, and an Innovation and Enterprise Fellow of the University of Oxford. She serves as a workshop committee member of the IEEE Engineering in Medicine and Biology Society Conference (EMBC), Neural Information Processing Systems (NeurIPS), International Conference of Machine Learning (ICML), and Prognostics and Health Management Conference (PHM).